OPTIMIZATION OF CHANNEL ESTIMATION FOR MIMO-OFDM NETWORKS

BY

AHMAD HASAN

A thesis submitted in fulfillment of the requirement for the degree Master of Science in Engineering

Kulliyyah of Engineering
International Islamic University Malaysia

AUGUST 2023

ABSTRACT

The 5th generation of cellular communication is a highly competitive market that promises some distinct features compared to the legacy LTE (long-term evolution) era. Some of these exclusive features include enhanced mobile broadband (eMBB), massive machine type communications (mMTC), and ultra-reliable low latency communication (URLLC) traffic (1 ms one-way latency, 99.999% reliability). Enabling these cutting-edge technologies requires a very smooth processing of user data and transmitted signals. Channel estimation and acquisition of channel state data is one of the important points in this regard because they can eventually enable signal transmission and subsequent processing. However, most of the estimators in research nowadays suffer from high complexity due to either too many constraints or conditions for unique solutions. This is already a significant problem in the communication industry because of its high dependency on resource allocation and system overhead. This research focuses on the enhancement of the legacy channel estimation processes to fit the 5G cellular standards. The industry standard Least Squares (LS) estimator was used as the basis for the optimized estimation. A dual residual function was enabled instead of a single one to make the estimator adaptive. Results show that making the weight function adaptive reduces the error at the receiver and provides a sharper response curve. A comprehensive study was carried out against the trending compressed sensing (CS) based semi-blind estimators as a second objective. And finally, the optimized algorithm was characterized on MIMO-OFDM systems to show its performance improvements in the cases of large arrays. These objectives were carried out through simulation, and results were constructively discussed based on the earlier points. Results were compared with parameters SNR, SER, PER, and BER. Some potentials regarding the channel estimation in MIMO-OFDM were left as pick-up points for future research interests.

ملخص البحث

يعتبر الجيل الخامس من الاتصالات الخلوية سوقًا تنافسيًا للغاية ، نظرًا لما يقدمه من بعض مقارنة بعصر LTE (التطور طويل الأمد) القديم.تتضمن بعض هذه الميزات الحصرية لشبكات الجيل الخامس النطاق العريض المتنقل المحسّن (eMBB) ، والاتصالات الضخمة من نوع الماكينة (mMTC) ، وحركة مرور اتصالات منخفضة زمن الانتقال فائقة الموثوقية (URLLC) (زمن انتقال أحادي الاتجاه يبلغ 1 مللي ثانية ، وموثوق(99.999٪).يتطلب تمكين هذه التقنيات المتطورة معالجة سلسة لبيانات المستخدم والإشارات المرسلة. يعد تقدير القناة والحصول على بيانات حالة القناة أحد النقاط المهمة في هذا الصدد. لأنه يمكن في النهاية تمكين إرسال الإشارة والمعالجة اللاحقة. ومع ذلك ، يعاني معظم في البحث في الوقت الحاضر من درجة عالية من التعقيد إما بسبب قيود أو شروط كثيرة جدًا للحلول الفريدة في صناعة الاتصالات بسبب اعتمادها على تخصيص الموارد وإدخال النظام. يركز هذا البحث على تعزيز عمليات تقدير القنوات القديمة لتلائم المعايير الخلوية لشبكات الجيل الخامس. تم إعطاء الأولوية لمنطقتين مختلفتين في هذه الدراسة ، أولاً ، تم تحسين المربعات الصغرى (LS) والحد الأدنى لمتوسط الخطأ التربيعي (MMSE) لإشارات 5G. تم تمكين وظيفة متبقية مزدوجة بدلاً من وظيفة واحدة لجعل المقدر متكيفًا. تظهر النتائج أن جعل وظيفة الوزن قابلة للتكيف يقلل من الخطأ في المستقبل ويوفر منحنى استجابة أكثر حدة. كهدف ثان ، تم إجراء دراسة شاملة لاستكشاف المقدرات شبه العمياء القائمة على الاستشعار المضغوط (CS). وأخيرًا ، تم تمييز الخوارزمية المحسّنة على أنظمة MIMO-OFDM لإظهار تحسينات الأداء في حالات المصفوفات الكبيرة. تم تنفيذ كل هذه الأهداف من خلال المحاكاة وتمت مناقشة النتائج بشكل بناء بناءً على النقاط المذكورة أعلاه. تمت مقارنة النتائج مع المعلمات SNR و SER و PER و BER. تركت بعض التوجيهات المتعلقة بتقدير القناة في MIMO-OFDM كنقاط التقاط للبحث في المستقبل.

.

AishA

DR. AISHA HASSAN ABDALLA HASHIM
Professor
Department of Electrical and Computer Engineering
Kulliyyah of Engineering
International Islamic University Malaysia

APPROVAL PAGE

I certify that I have supervised and read this study and that in my opinion, it conforms to acceptable standards of scholarly presentation and is fully adequate, in scope and quality, as a thesis for the degree of Master of Science in Engineering

……..
S. M. A. Motakabber
Supervisor

……..
Mohamed Hadi Habaebi
Co-Supervisor

……...
(For) Farhat Anwar
Co-Supervisor

This thesis was submitted to the Department of Electrical and Computer Engineering and is accepted as a fulfilment of the requirement for the degree of Master of Science in Engineering

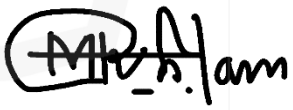

……..
Md. Rafiqul Islam
Head, Department of Electrical
and Computer Engineering

This thesis was submitted to the Kulliyyah of Engineering and is accepted as a fulfilment of the requirement for the degree of Master of Science in Engineering

……..
Sany Izan Ihsan
Dean, Kulliyyah of Engineering

DECLARATION

I hereby declare that this dissertation is the result of my own investigations, except where otherwise stated. I also declare that it has not been previously or concurrently submitted as a whole for any other degrees at IIUM or other institutions.

Ahmad Hasan

Signature  Date .....28-6-2023.....

INTERNATIONAL ISLAMIC UNIVERSITY MALAYSIA

DECLARATION OF COPYRIGHT AND AFFIRMATION OF FAIR USE OF UNPUBLISHED RESEARCH

OPTIMIZATION OF CHANNEL ESTIMATION FOR MIMO-OFDM NETWORKS

I declare that the copyright holder of this thesis is Ahmad Hasan

By signing this form, I acknowledge that I have read and understand the IIUM Intellectual Property Right and Commercialization policy.

Affirmed by Ahmad Hasan

……..…….. …….28-6-2023……..

Signature Date

ACKNOWLEDGEMENTS

All Praise Be To Allah, The One And Only Worthy.

It's his blessing that led me to the completion of this lengthy work. Truly his bounties are limitless.

I am truly indebted to my supervisor, Assoc. Prof. Dr S. M. A. Motakabber, without his guidance and support, this thesis work wouldn't be a reality. I appreciate his willingness always to help me, and most notably, his directness towards the suggestions. His experience in engineering research helped me a lot towards avoiding mistakes that otherwise would be inevitable. He was kind enough to make time for me whenever I was in need of some professional tips or suggestions. His insights into problem-solving techniques and troubleshooting were very commendable. I also feel indebted to both of my co-supervisors, Prof. Dr. Farhat Anwar and Prof. Dr. Mohamed Hadi Habaebi. They also provided me with consultancy whenever I needed it.

Lastly, and most importantly, my gratitude also goes to my beloved wife-to-be.

Once again, we glorify Allah for his endless mercy on us, one of which is enabling us to successfully round off the efforts of writing this thesis. Alhamdulillah

TABLE OF CONTENTS

LIST OF TABLES

LIST OF FIGURES

LIST OF ABBREVIATIONS

BS	Base station
CE	Channel estimation
CP	Cyclic prefix
CSI	Channel state information
FBMC	Filter bank multi-carrier
F-OFDM	Filtered orthogonal frequency division multiplexing
IFFT	Inverse fast Fourier transform
FFT	Fast Fourier transform
MIMO	Multiple input, multiple outputs
MMSE	Minimum mean square error
MSE	Mean square error
OFDM	Orthogonal frequency division multiplexing
LMMSE	Linear minimum mean square error
LOS	Line of sight
LS	Least squares
UE	User equipment

LIST OF SYMBOLS

η	White noise
H	Channel impulse
β	Path loss
U	Uniform distribution
γ	Signal to noise ratio

CHAPTER ONE

INTRODUCTION

1.1 BACKGROUND

The 5th generation of the mobile system era promises a lot of enabling technologies that are supposed to take the legacy LTE standards to a whole new level. Some of the few groundbreaking properties of this cellular system include Enhanced Mobile Broadband (eMBB), Massive Machine Type Communications (mMTC) and Ultra-Reliable Low Latency Communication (URLLC, <1ms) (Shafi et al., 2017). To enable these cutting-edge features, the next-generation cellular system will adopt a few new technologies and amendments (Beltran, Ray, & Gutiérrez, 2016). One of the most critically acclaimed ones is the millimetre wave (mmWave) Massive MIMO system, which lies in the vast range of 30Ghz-300Ghz (Rappaport et al., 2017). This technology's key features include elevated user throughput and enhanced spectral and energy efficiencies. Not to mention the increase in the capacity of mobile networks through the joint capabilities of the ultra available bandwidth in the mmWave frequency bands and high gains using new techniques as spatial multiplexing obtained via massive antenna arrays (Rappaport et al., 2017).

Although the potentials of what could be gained in the mmWave range are promising, the difficulties in building and sustaining such an infrastructure are also very demanding (Xiao et al., 2017). Nevertheless, much research has already been conducted, and even more proposals regarding the solutions are starting to arise. One of the major considerations among these is the Ultra-Dense Network or UDN (Kamel, Hamouda, & Youssef, 2016). It refers to the ultra-dense deployment of the small-scale BS within the coverage of bigger cell BSs. The cell types are classified as metro, micro, pico or femtocell in a decreasing manner.

The Massive MIMO is another major part of this new generation of cellular communication schemes. It is characterized by increasing the number of antennas for transmission and reception several times (Buzzi et al., 2016). Clearly, this intends to

achieve the already discovered benefits of the MIMO on a large scale. Using spatial multiplexing can enhance the capacity of the current cellular infrastructure (D. Liu et al., 2016). The large number of available degrees of freedom through numerous antennas can improve spectral efficiency. With the help of hybrid beamforming, further reduction in interference is possible (Ahmed Alkhateeb & Heath, 2016). It also helps reduce latency, one of the three major targets. The full benefit of Massive MIMO is only obtained when it's deployed in the aforementioned mmWave region. Because of the small size of the apertures, low power-consuming components and avoiding costly non-linear A/D converters, a cost-efficient infrastructure is possible (Hemadeh, Satyanarayana, El-Hajjar, & Hanzo, 2018). The maximum benefits for mmWave Massive MIMO are feasible, provided that different antenna pairs at the transmitter and the receiver undergo independent fading channel characteristics. For this, the antenna elements are spaced at $\leq 0.5\lambda$, which gets even smaller as we go deep in the mmWave region. Apparently, this allows for more antenna elements to be placed in close vicinity of each other. The feasibility of optimal performance is also heavily dependent on the availability of the CSI, which is the task of the channel estimation portion. Because the contribution of channel estimation is crucial for the receiver, this section is discussed separately at the end of this chapter.

However, small apertures mean low radiation power and, thus, high attenuation (Ghosh, Maeder, Baker, & Chandramouli, 2019). Therefore, mmWave systems must have antenna characteristics of high directivity, configurable, etc. But since this brings up the question of the economic viability, an alternative and even more promising aspect of the 5th generation cellular system comes into focus: the contribution of hybrid beamforming or precoding (Ahmed et al., 2018). But since that is another major area of the current research and also out of the scope of this work, we won't discuss it any further here.

Since the no of antennas at the BS increases exponentially at mmWave, the channel characteristics turn deterministic, and the channel orthogonality becomes asymptotic (Zhang, Ge, Li, Guizani, & Zhang, 2017). So, the no of UE that can be supported simultaneously decreases owing to fluctuating coverage area. The path-loss models for mmWave also show an increased degree of moderate path-loss, and the NLOS signals become more vulnerable to obstacles like solid bodies and buildings (i.e.

less penetration power) (Hong, Baek, & Ko, 2017). It is due to the smaller size of the wavelength compared to the obstacles. So the signals in this frequency range are more vulnerable to shadowing, diffraction, blockage etc.

Signal processing in mmWave is far more challenging than that of μWave. It's largely because of the increasingly random signal in this frequency range (Sun et al., 2016). Various models have been proposed assuming different criteria to characterize the signal behavior in mmWave effectively. Reportedly these models usually perform well to delineate a certain parameter while considering the behaviour of other parameters constant. However, since the performance parameters of signal in mmWave, like the attenuation is, random and heavily dependent (correlated) on other relevant parameters, it's far more challenging to characterize the behaviour of signals in this frequency range (Hemadeh et al., 2018; B. Wang et al., 2018).

The 3GPP has taken some new initiatives to alleviate this problem. For instance, starting from release 15, the available bandwidth is divided into two frequency ranges, namely FR1(<6Ghz) and FR2(23Ghz-53Ghz). For FR1, both TDD and FDD duplexing methods are being deployed, while in the higher frequency range FR2, only TDD is available for now. The subcarrier spacing in these ranges can be a power of two multiple of 15kHz or (2n×15kHz). Also, for the new release, the frame structure is renewed too. For instance, newer units like Bandwidth Parts(BWP) are being utilized further to facilitate the UE configuration to the BS.

The smallest physical resource is the resource element in the 5G New Radio (5G NR). Unlike the legacy LTE configuration, the Resource Blocks or RBs that carry these resource elements are evaluated in the frequency domain only. Precoding in mmWave is of even more importance than it was for LTE since the attenuation in mmWave is heavily dependent on beam steering and alignment (Sohrabi & Yu, 2017; Venugopal, Alkhateeb, Gonzalez Prelcic, & Heath, 2017). In addition, newer multiplexing techniques like Filtered-OFDM or F-OFDM are being considered, further dividing the band into subbands for more configurability. As it stands now, one of the major problems with the fifth generation of cellular networks will surely be the 'complexity'. It's clear from the already published numerous studies that the system overhead or complexity is increasing with leaps and bounds to make the new 5G era more

configurable and user-friendly. So, the researchers also consider simplicity to balance the trade-off between features and resource allocation. It is one of the reasons for this study to optimize and, more importantly, to make the estimation of channel parameters more resource friendly and thus aid in less complex and more feature-friendly cellular communication.

1.2 PROBLEM DELINEATION

The channel estimation or the process of acquiring CSI (Channel State Information) is increasingly difficult in the 5G domain mainly due to the vast amount of instantaneous data to process and a pre-beamforming low SNR (Qin, Gui, Cheng, & Gong, 2018). But to reap most of the benefits from hybrid precoding, which is being well investigated at the moment, an efficient channel estimation (CE) algorithm is crucial. Without a substantially accurate knowledge of CSI, the accuracy of the precoding is very limited. Thus, these two aspects of signal processing are of great importance at the moment, and a lot of studies are focusing on a joint evaluation of hybrid precoding and estimation algorithms. Due to the numerous no of antennas and the large dimension of the channel matrix, the calculations required to determine the channel parameters are almost exponentially difficult. Owing to a high no of degrees of freedom, researchers are trying to exploit that the transmitted signal in mmWave is sparse in some domains. This lead to the idea of compressive/compressed sensing (CS) theories that involve representing the channel matrix in a domain in which most of its elements are sparse or zeros, thus reducing the number of calculations. Through this sparse representation, CS theories allow a signal to be sampled at a rate far lower than that required by the Nyquist criterion. But current CS algorithms present some complexity as most of these algorithms are NP times hard to compute. Even so, the CS methods are certainly one of the leading candidates for the CE process as it dramatically reduces the no of parameters to be estimated (Uwaechiaet al., 2019). Some of the recent research for the mmWave channel estimation assumes perfect CSI at the transmitter or CSI-Tx (Ahmed Alkhateeb et al., 2014; Dai et al., 2019; Uwaechia et al., 2019), which is itself, a potential topic for further exploration. On the other hand, some works took a more practical approach by assuming partial CSI knowledge at the transmitter (A. Alkhateeb et al., 2013). Another portion of the research on estimation in mmWave focused on determining the angle of

arrival (AoA) and angle of departure (AoD) efficiently by presenting them as a sparse recovery problem and then proposing greedy or other types of algorithms to solve it.

So few of the significant problem regarding the estimation performance, such as complexity, applicability and the role of channel statistics, are still at large and requires further study for the 5th generation of mmWave cellular networks.-

1.3 RESEARCH OBJECTIVES

The intentions behind this work can be broadly put into three sections:

1. To Optimize the conventional training algorithms: As found in the literature, using static weights and a non-adaptive scheme reduces the efficiency of the legacy algorithms like LS. The first objective is to eliminate this problem by switching to a dual residual scheme.
2. To Adaptively estimate channel based on the Characterization of the new algorithms on MIMO-OFDM systems: This study is based on the MIMO-OFDM system; hence the results will reflect the effect of the proposed algorithm on a standard MIMO-OFDM system. The results are shown as criteria such as BER, SER, PER etc.
3. To evaluate Performance evaluation against trending CS-based methods: Compressed sensing-based methods are trending because of their efficiency. The last objective is to analyse the performance of the proposed algorithm against the benchmark CS one to show the superiority of the optimized LS method.

1.4 SCOPE OF THE RESEARCH

This research work is intended to be done with computer simulation software. We plan to utilize Matlab as the primary simulation platform. With the help of a communication toolbox to facilitate the new subchannel construction and thus run simulations according to the optimized algorithms. The simulations will be run in an x64-bit program, and the codes of the simulations can be found in the Appendix. Note that since the simulations

involve multiple criteria evaluation, the simulation parameter may be changed from code to code. It is intended to present the simulation results in terms of bit error rate (BER), mean square error (MSE), symbol error rate (SER) and or throughput. This research doesn't involve any experimental data; thus, no apparatus or machine outside the computer software will be used.

1.5 ORGANIZATION OF THE THESIS

This thesis work is divided into six chapters. The first chapter is this one. The subsequent chapters are the literature review, methodology, paradigm, results & discussion and conclusion. Below is a short note on each of the containing chapters of this thesis-

Chapter 1: Contains the preface of the thesis and the organization of the rest of the chapters.

Chapter 2: Entails the studies used for this thesis work. It also discusses the features and limitations of this research and the research work(s) used for benchmarking this thesis.

Chapter 3: The methodology chapter briefly compares the techniques used for the research works stated in Chapter 2. Discusses their potential benefits and limitations and, based on these observations, derives the scheme(s) used to obtain the objectives of this research.

Chapter 4: Defines the setup of this thesis work, including method of obtaining results, simulation environment and method, type of statistical analysis used etc. Note that this thesis work is entirely simulation-based, but data outside the simulation environment may be added if necessary. The chapter includes the results obtained via simulation and compares them for benchmarking. It also demonstrates how the objectives are achieved and the amount of improvement done.

Chapter 5: The final chapter of this thesis deals with the conditions of the target objectives of this thesis. It also discusses the problems faced during the pursuit of the goals and also sheds light on the potential research objectives for the following

1.6 CHAPTER SUMMARY

The significance and contributions of this research have been demonstrated in this chapter. The existing problems and their potential solutions were also discussed. The intentions behind this study and possible outcomes were presented. Quick takeaways from the literature review have been proposed as a summary. The scope of the research has also been looked upon. At the end of the chapter, an outlook and total overview of the thesis have been summarized. Furthermore, what this study is about and limited to is also discussed.

CHAPTER TWO

LITERATURE REVIEW

2.1 INTRODUCTION

Much work has been done through the years in signal processing for cellular networks (Zhang, Ge, Li, Guizani, & Zhang, 2017). Especially starting from the LTE era, the process of acquiring channel state information or CSI, known as channel estimation, has gained immense attention due to its ability to reduce the overhead to the system and increase the throughput. The CSI is usually estimated at the receiver and fed back to the transmitter unless otherwise specified. Although the CSI feedback system is also an integral part of the estimation procedure, most research regarding channel estimation doesn't explicitly provide any feedback algorithm since the amount of feedback is generally kept very small and tolerable for most OFDM systems. That being said, for the 5th generation cellular network, it's said that with an increased no of antennas (Massive MIMO), the feedback amount is expected to increase substantially. However, it's not a part of this study.

There are three types of conventional channel estimation procedures; Blind, Semi-blind & training/pilot based. Of these three, the semi-blind and especially the pilot-based channel estimations have gained popularity due to their flexibility and robustness against errors. Most widely researched pilot-based estimation techniques include the least square (LS) method, the Minimum Mean Squared Error(MMSE) method, and the Linear MMSE (LMMSE). There are, however, some other lesser-known modifications of these methods like Normalised Least Mean Square (NLMS) and Recursive Least Squares (RLS) (Masud & Kamal, 2010), Space Alternating Generalized Expectation-maximization (SAGE) (Ketonen, Juntti, Ylioinas, & Cavallaro, 2013), Iterative-Compensated MMSE (IC-MMSE) (Y. Liu & Sezginer, 2011) and so on. All these modified algorithms have in common that the researchers added weighted values, statistical info or similar criteria to make up for certain drawbacks in these proposed algorithms. For instance, adding further taps in the LS algorithm can decrease the estimation errors (Van de Beek et al., 1995), which led to numerous variations in these algorithms. This study intends to discover the appropriate

approaches to these modifications that will suit the mmWave MMIMO OFDM systems. Despite being old, these algorithms are still large in practical cellular networks. They arguably can have the same amount of contribution to the 5th generation of cellular networks as any other new contenders like the compressed sensing (CS) algorithms. Which we shall focus on as another objective of this study.

The rest of this chapter is assembled as follows; First, a short history of pilot/training-based estimation is given, followed by the current trends in this domain and finally, the existing research gap. Next, a brief introduction to compressed sensing (CS) based theories is given along with current works in this manner. The CS section is kept short since optimising them in this study is not our concern; they'll be used to characterize the performance trade-off with overhead in contrast to the pilot-based estimations. The final section of this chapter will include a comparative demonstration of different trending algorithms, their limitations and possible amelioration. Finally, the chapter will be concluded with a brief summary.

2.2 PILOT-TRAINING-BASED CHANNEL ESTIMATION

As mentioned in the introduction, pilot-based channel estimation involves determining the channel impulse response in the frequency domain with the help of a set of predetermined symbols. The impulse response is selected from the knowledge of the received symbol matrix and the pilot symbols. There are three pilot structure types: block, comb, and lattice. Block type involves inserting the pilot symbols for all the subcarriers for a particular instant and then sending them periodically. So, this type of pilot training is helpful for slow-fading (frequency selective) channels.

On the other hand, comb-type pilots are useful for fast-fading channels since pilots are inserted following the time axis. In the lattice-type pilot, symbols are inserted in both time and frequency axes to ease interpolation. A generalized picture can be comprehended from Figure 2.1.

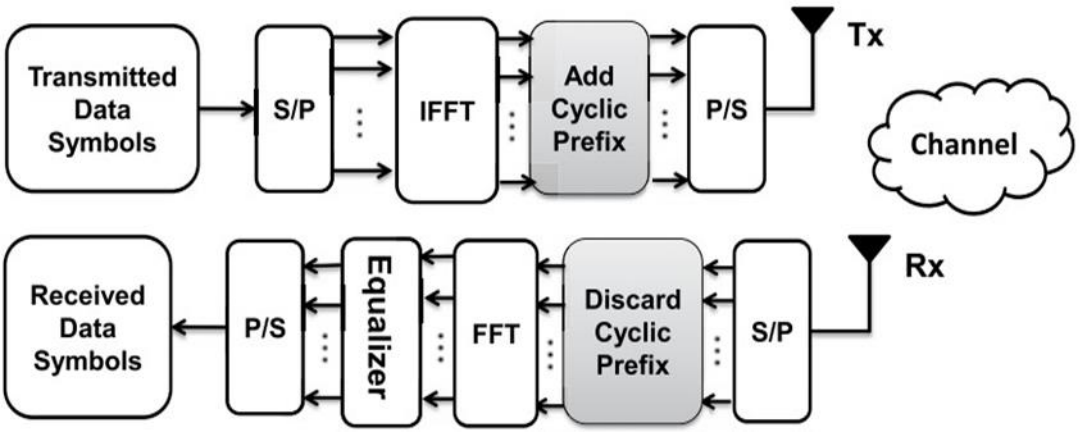

Figure 2.1 Organization of a general OFDM system (Hamamreh et al., 2018)

Pilot-based channel estimators are highly adjustable because of their simplicity. And any additional available info can be added to each iteration step to stretch the performance boundary further. In light of these features, the literature discussed in this chapter mainly focuses on pilot-based training. A short comparison of the differences in signal processing between microwave and millimetre waves is given in Table 2.1.

Table 2-1 Comparison between µWave and mmWave

Parameters	**µWave**	**mmWave**
Gain	Larger	About the order of two times smaller.
Path loss	Lower for a certain BS-UE distance.	Higher than µWave for a certain BS-UE distance.
Shadowing	Small and independent of blockage and NLOS propagation.	Larger than µWave and dependent on several random variables also affected by blockage and LOS/NLOS propagation.
Interference	They are affected by proximity, distance-dependent and result in background interference for increasing no of interferers.	High-attenuation by blockage and antenna gain patterns obscure in terms of distance and demonstrates

		an ‘On-Off’ kind of behaviour.
SINR	They are affected by proximity and distance-dependent, resulting in background interference for an increasing number of interferers.	High-attenuation by blockage and antenna gain patterns obscure in terms of distance and demonstrates an ‘On-Off’ kind of behaviour.
Antenna array conFigureuration	The BS side has massive arrays.	Both the BS and UE have massive antenna array capacities.
DSP	Moderate level of complexity.	Highly complex
Call handover	It is generally done at the cell perimeter, less frequently.	More frequent due to susceptibility to blockage, beamforming etc.
Gain	Larger	About the order of two times smaller.
Path loss	Lower for a certain BS-UE distance.	Higher than µWave for a certain BS-UE distance.
Shadowing	Small and independent of blockage and NLOS propagation.	Larger than µWave and dependent on several random variables also affected by blockage and LOS/NLOS propagation.
Interference	They are affected by proximity and distance-dependent, resulting in background interference for the increasing number of interferers.	High-attenuation by blockage and antenna gain patterns obscure in terms of distance and demonstrates an ‘On-Off’ kind of behaviour.
SINR	Has a more lenient change from the cell centre to the cell perimeter.	Suffers from rapid random fluctuations caused by blockage, efficiencies of

		beam alignment and steering.
Antenna	The BS side has massive arrays.	Both the BS and UE have massive antenna array capacities.
DSP	Moderate level of complexity.	Highly complex
Call handover	It is generally done at the cell perimeter, less frequently.	More frequent due to susceptibility to blockage, beamforming etc.

2.3 CONTEMPORARY WORKS AND RESEARCH GAPS

Although conventional channel estimation methods have been the topic of interest for a very long, the study behind them hasn't waned in recent years. Introducing new statistical techniques like the Compressed Sensing (CS) based methods have sparked a new interest in the tradeoff in performance and simplicity between these two domains of channel estimation algorithms. Although we're primarily focusing on LS and MMSE-based methods, this research's secondary objective is to find the performance gap between this trending CS domain and the conventional channel estimation methods.

2.3.1 Channel estimation in FBMC Systems

The Filter Bank Multicarrier (FBMC) system is an emerging technology that is supposed to mitigate some existing concerns in the OFDM systems, like out-of-bound (OOB) radiations and uplink synchronization errors. It is an adjustment of OFDM and targets to overcome some of its limitations, albeit at the cost of increased signal processing. FBMC boasts some improvements in efficient BW utilization because of the redundancy of CP, spectrum efficiency and the allocation for robust narrowband jammers. At the same time, it imparts the difficulties of sensitive synchronization issues and very complex signal processing requirements. But because of its features, it's being increasingly studied in contemporary signal processing works. For instance, judging the effects of timing and frequency offsets in mmWave signal processing is very important. Because the successful recovery of the transmitted symbols greatly depends on it. It's

found in the studies of (Aminjavaheri et al., 2015) that if we assume an ideal channel response and ignore the fading effect, the transmitted data symbols can be presented as-

$$\hat{X}_{mk}^{(l)} = \langle y(t), h_{mk}(t) \rangle \quad (2.1a)$$

$$= X_{mk}^{(l)} + I_{MAI} + \eta \quad (2.1b)$$

where $h_{mk}(t)$ denotes the receiver basis corresponding to the (m, k) time-frequency point, I_MAI is the multiple access interface if the waveform is non-orthogonal, and η is the associated noise. From equation (2.1b), it can be seen that the transmitted symbols for the lth user can be estimated whether the waveform is orthogonal like OFDM, FDMA or non-orthogonal like GFDM (Generalized Frequency Division Multiplexing).

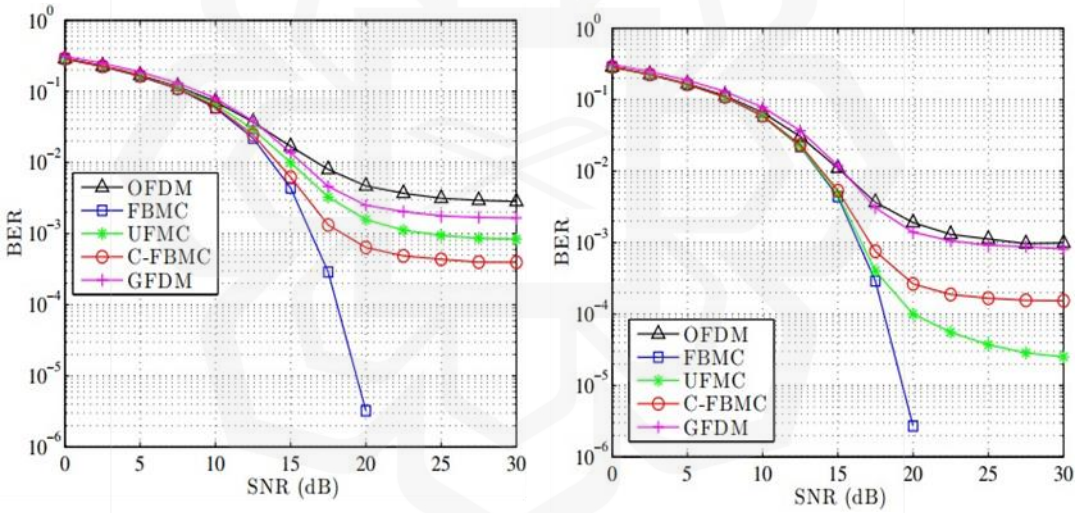

Figure 2.2 BER performance of different waveforms depending on TO and CFO differences and user synchronization (Aminjavaheri et al., 2015)

One can easily comprehend the performance upper hand of FBMC from Figure 2.3. A smooth-edge windowing algorithm should be implemented on both the transmitter and receiver sides to reduce sensitivity caused by timing offset and carrier frequency offset (CFO). Since we can see the difference when users are quasi-synchronized, they're TOs in the range of CP.

FBMC with Offset QAM (OQAM) shows great potential using sharp pulse shaping filters in both frequency and time domains. In their work (Singh et al., 2019), the authors presented the conventional semi-blind, training-based and data-aided channel estimation schemes for the FBMC, as mentioned earlier, which are still popular choices for the OFDM-based systems. Their work showed that semi-blind estimation schemes with OFDM-FBMC perform better than the same system using pilot-training-based estimation (Singh et al., 2019). They also show that although using second-order channel statistics can significantly increase system overhead, it contributes to a lesser MSE. In the presence of channel estimation errors, they derived
the expression for BER of their MIMO-FBMC system as,

$$\bar{P}_b \cong \left[\frac{1}{2}(1-\mu_0)\right]^{D+1} \sum_{q=0}^{D} (D+ql)\left[\frac{q}{2}(1+\mu_0)\right]^{q} \tag{2.2a}$$

where the $\mu_0 = \sqrt{\frac{\bar{\gamma}_{\bar{m},\bar{n}}}{2+\bar{\gamma}_{\bar{m},\bar{n}}}}$ is dependent on the post-processing SNR $\bar{\gamma}$. and D is the difference between no of transmitted symbols and no of received symbols. They also included a comparison of overhead between different estimation schemes. From equation (2.2a), it's evident that the secret behind a better estimator lies withing the maximization of μ_0 or the post-processing SNR.

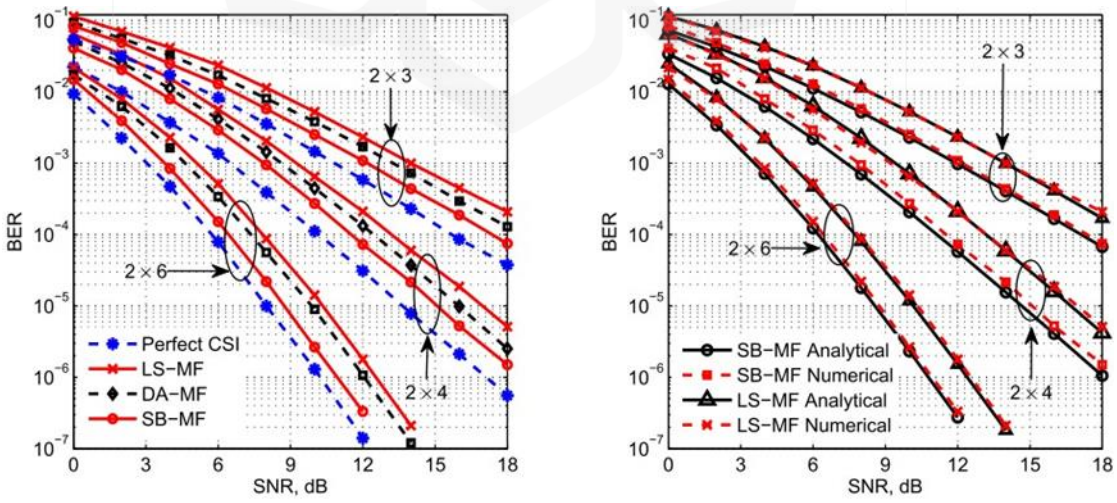

Figure 2.3 Performance upper hand of the semi-blind MIMO-FBMC and data-aided MIMO-FBMC over conventional least squares MIMO-FBMC (Singh et al., 2019)

Figure 2.3 shows that semi-blind FBMC has the best performance among different MIMO systems because of the use of second-order channel statistics and is very close to the one where a perfect CSI is assumed. Furthermore, the FBMC system has the advantage of being more spectrally efficient. Because cyclic prefixes (CP) are redundant for this system, the authors emphasized that using the data-aided estimation, channel statistics, and training symbols yields better BER performance for the MIMO-FBMC system as compared to the conventional LS methods that only rely on the pilot training.

This work insinuates that the OFDM estimation performance in terms of BER can also be enhanced if data-symbol estimates are used besides the training symbol estimates. In light of this, the simple conventional estimates like the LS can be further adjusted for Massive MIMO if the data-symbol estimates are considered in the algorithm.

2.3.2 Channel estimation with GSM

Spatial modulation (SM) is a modulation technique that uses only one transmit RF chain and one antenna element in a multiple transmit antenna array and thus sends the information symbol through the chosen antenna. It means less inter-antenna synchronization, less hardware complexity and, in a sense, less cost for a transmitting system. General Spatial Modulation, or GSM, is an extension or generalization of this idea that enables multiple transmit antennas to be active simultaneously. Thus GSM can allow much higher data rates which come with the cost of adequately detecting the signal at the receiver. Numerous researchers are working on finding low-complexity detection schemes which are essential in the case of GSM because of high transfer rates.

Thus, Massive MIMO systems with GSM are a promising area of channel estimation research. Spatial modulations have been shown to have some attractive characteristics over conventional modulation schemes like reduced power consumption, redundancy of antenna synchronization and cancellation of inter-antenna interference. Exploiting the system's double-sparsity and using compressed sensing algorithms can also lead to better performance than conventional blind and semi-blind algorithms (Kuai et al., 2019). The blind CE estimates the channel offset on the signal without

using any pilot signal. So if *H* is the impulse response of the channel, *X* is the transmitted symbols, then the blind estimation problem for the observed data matrix *Y* can be summarized as,

$$(\widehat{H}, \widehat{X}) \quad = \arg max_{H,X}(X, H|Y) \tag{2.3a}$$

The parameters in (2.3a) are used in blind and semi-blind algorithms to devise various estimators. The angle of arrival, or AoA, it's estimated using the following expression-

$$\sin\theta_q \quad = \sin\vartheta_q^{DFT} + \varsigma_q\,; \quad where\ \varsigma_q \sim U\left[-\frac{1}{2\acute{M}}, \frac{1}{2\acute{M}}\right] \tag{2.3b}$$

Here ϑ_q^DFT is the DFT sampling grid. and U are denoting the uniform distribution. Based on this, different types of blind and semi-blind algorithms can be devised.

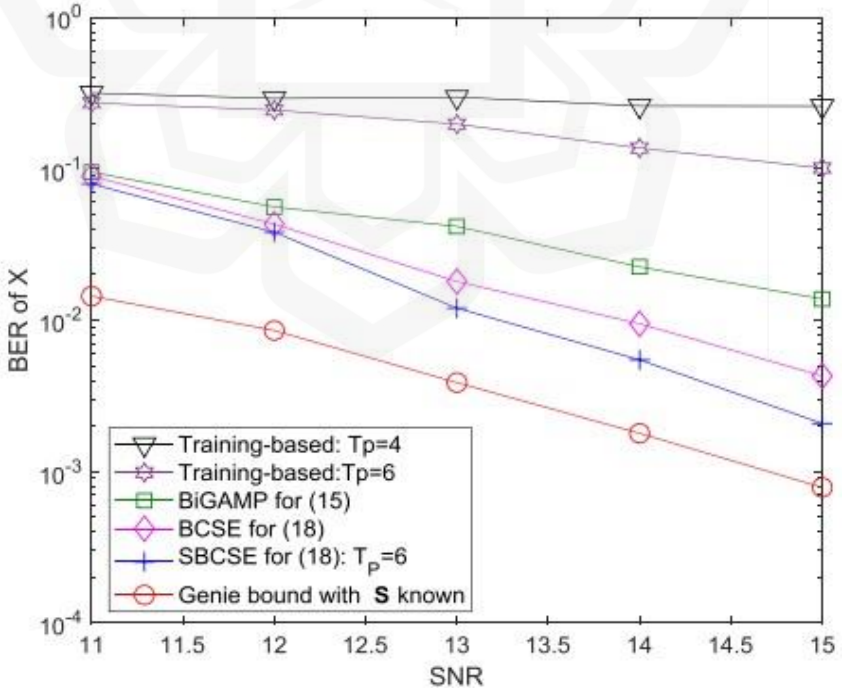

Figure 2.4 BER performance of different schemes using GSM in large-scale fading (Kuai et al., 2019)

GSM allows multiple antennas to be active simultaneously and thus send multiple symbols at the same time to different users. Double sparsity is often exploited in contemporary articles for channel estimation, which means both the clustered channel sparsity in the angular domain and the inherent sparsity of the signal in spatial modulation are accounted for. Blind and Semi-blind detection algorithms show increased efficiency in spatially modulated systems if substantially accurate channel statistics are available

Exploiting the signal's sparsity has led to numerous channel estimation methods, like compressed sensing. However, especially for the problem of multiuser detection, some studies have shown that utilizing random and structured sparsity learning algorithms makes it feasible to get better results than pilot symbols, albeit with increased complexity to some extent. The significant difference between structured and random sparsity is that in random sparsity, the entries of the transmitted signal matrix are independent, whereas, in structured sparsity, it's highly specific; that is, each row of the transmitted signal matrix X corresponds to only one active packet in the observation window (Bjornson et al., 2017; Ding et al., 2019; Zhang et al., 2018).

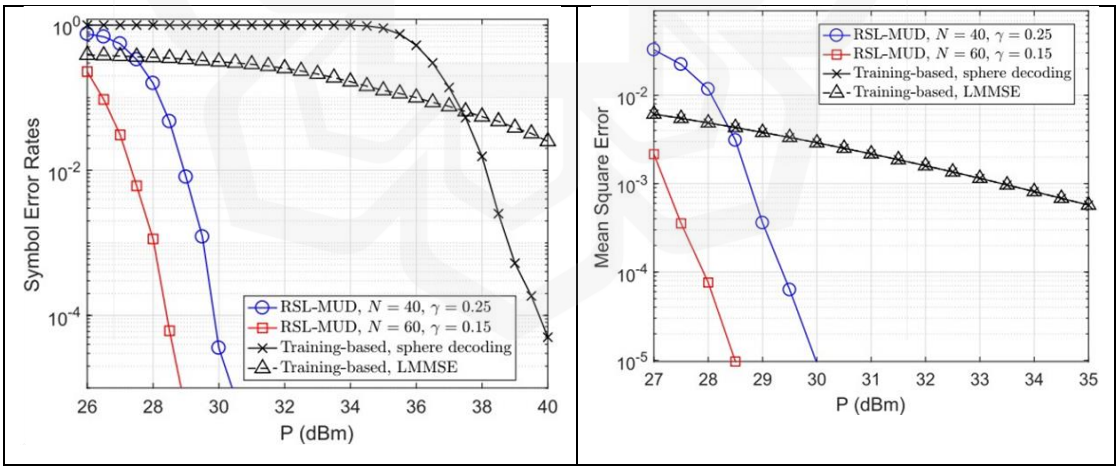

Figure 2.5 SER & MSE for random sparsity-based estimation vs training-based estimation (Ding et al., 2019)

However, in systems like Massive MIMO, where numerous antennas are applied, the channel statistics' availability, processing and accuracy are also of great concern. Even though methods like the Semi-blind algorithms have superior

performance over the conventional training-based methods, the adjustment of the channel statistics in these algorithms puts another restrain on the estimation algorithm. In training-based methods, this complexity is avoided.

A recent study by Pan et al. (2019) showed that evaluating the channel estimation and decoding performance together can enable a good overview of the overall BER performance of the OFDM system (Pan et al., 2019).

The authors demonstrated the performance of joint ML(Max Likelihood) decoding, conventional mismatched ML decoding and a novel scheme of what they call as separate ML decoding along with the addition of MMSE channel estimation.

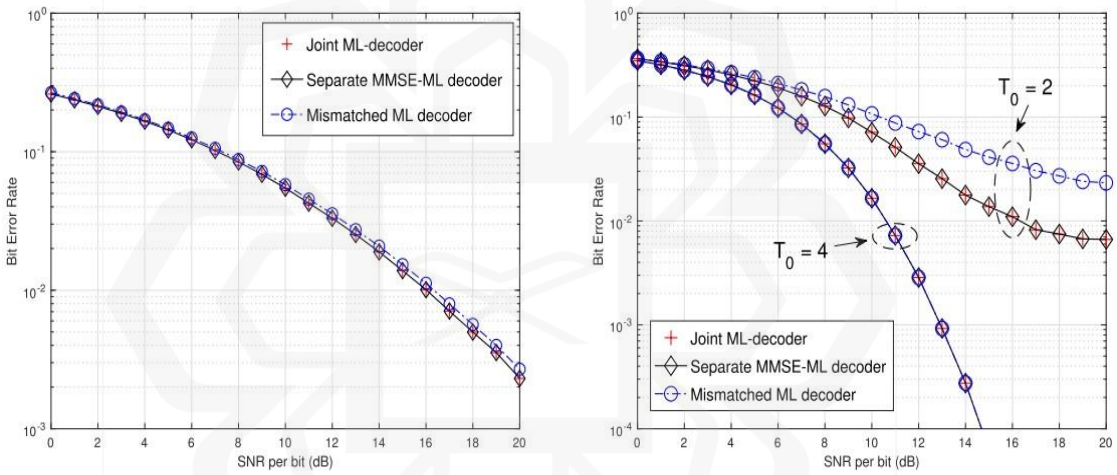

Figure 2.6 BER vs SNR performance when 16QAM(Left) and QPSK(Right) modulation is used with joint estimation

They used two modulation schemes, 16QAM and QPSK, to show the performance overview. Figure 2.2 shows that the BER performance achieved by the joint ML-decoder is identical to that achieved by the separate MMSE-ML decoder. Also, the joint *ML* decoder and the separate MMSE-ML decoder marginally outperform the mismatched *ML* decoder. They mathematically proved that these two detection schemes are identical in terms of performance, although conventionally, it's thought that joint detection schemes are superior. A possible reason can be the estimation error in the separate decoding scheme. They also showed that MMSE algorithms have the best performance in terms of overall system efficiency.

Nevertheless, another potential candidate for this purpose can be the LS estimate since it has the advantage of simplicity over the MMSE method. Although the MMSE method yields better results when accurate secondary channel statistics are available, resource friendliness can be crucial when a complex system like Massive MIMO is considered.

The increase in wireless communication entities also paves the way for security issues like eavesdropping and spoofing. Pilot Spoofing Attack (PSA) happens when an eavesdropper sends an identical pilot as the legitimate user. In these security issues, accurate CSI through channel estimation is paramount. The pilot spoofing attack (PSA) happens during the uplink pilot training phase. A combined baseband is usually considered at the BS to incorporate the compromised pilot with the legitimate one (W. Wang et al., 2019).

$$\boldsymbol{Y_p} = \sum_{k-1}^{K} \left(\sqrt{P_u \beta_{u_k}} \boldsymbol{h}_k^H \boldsymbol{s}_k + \sqrt{P_e \beta_{e_k}} \boldsymbol{g}_k^H \boldsymbol{s}_k \right) + N \tag{2.4a}$$

Where *P, β, h, g* and s mean the signal's power, path loss, and small-scale Rayleigh fading of the user and the attacker and the pilot signal, respectively. The notations *u* and *e* mean the user and the eavesdropper, respectively. N is used to incorporate AWGN. Then by using the process of elimination on equation (2.4a), it is shown that the MMSE estimator of the contaminated signal block unit can be expressed as,

$$\hat{\boldsymbol{h}}_k = \frac{\sqrt{P_u \beta_{u_k}}}{\Sigma} \boldsymbol{y}_k + \frac{P_u \beta_{u_k}}{\Sigma_k} \boldsymbol{h}_k + \frac{\sqrt{P_u P_{e_k} \beta_{u_k} \beta_{e_k}}}{\Sigma_k} \boldsymbol{g}_k + \frac{\sqrt{P_u \beta_{u_k}}}{\Sigma_k} \boldsymbol{n}_k \tag{2.4b}$$

One can easily distinguish between the legitimate user and the eavesdropper from equation (2.4b). The result of this smart separation is also apparent as the CSI of the legitimate user can be obtained with even more accuracy, as can be seen from Figure 2.3 (W. Wang et al., 2019).

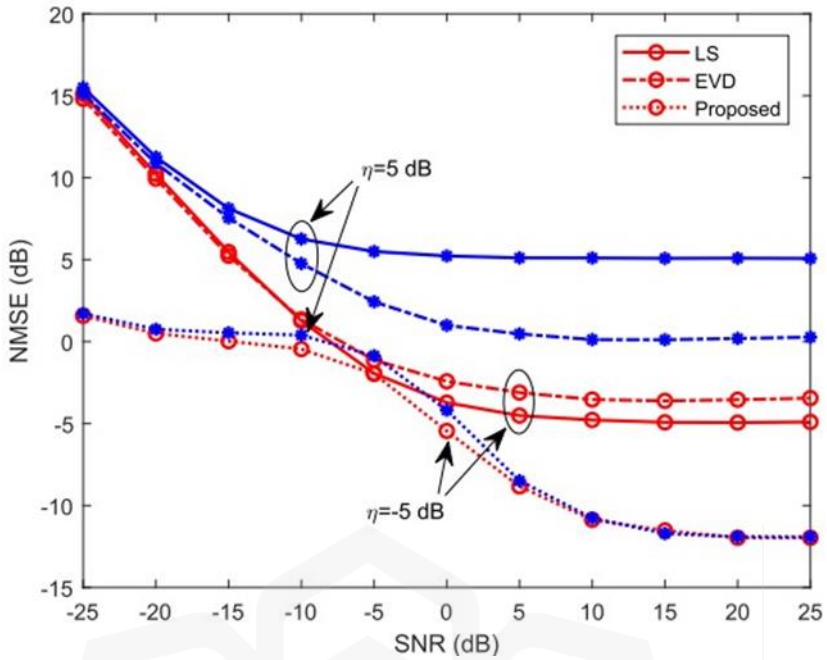

Figure 2.7 NMSE of different channel estimators where N = 64 and K =4

The authors showed that it's comparatively easy for eavesdroppers to 'spoof' or copy the training sequence from the BS and send an identical but malicious copy to the MU. It can dramatically reduce the link quality and not to mention the safety of the info concerning MU. Moreover, this physical layer security breach can rapidly fluctuate degrees of freedom (DoF) to zero (Basciftci et al., 2018). To figure out this kind of pilot spoofing attack in TDD systems, the authors proposed a two-step channel training-based estimation scheme that first detects the attacker's presence and then effectively separates the contaminated data bits of the training sequence from the ones that the BS sends. The authors also derived a lower bound on a max achievable uplink and downlink 'secrecy' rate. Later, the estimation errors arriving from using a limited number of samples and antennas were also calculated, and an estimate of the achievable improvement under MMSE precoding was derived. The authors showed enhanced performance of their double training scheme in terms of normalized MSE (NMSE).

This double training scheme can be applied, and its performance bound on the max achievable uplink-downlink rate can be studied for the multi-cell Massive MIMO. Also, a parallel NMSE account can be derived for the LS and other conventional estimation schemes.

Molecular communication (MC) is a recent invention focusing on communicating among medical apparatus and nanorobots. In MC, the bio-nanomachines are the entities that communicate as transmitter and receiver. To transmit the molecules, they need a liquid or gaseous medium. Thus these kinds of systems are often called 'Diffusive' systems. The channel estimation, equalization and detection of such a Diffusive MIMO or DMIMO system are studied (Mohammadreza Rouzegar & Spagnolini, 2017). They derived training-based estimation schemes and decision-based feedback equalizers for the DMIMO system. Since the transmission of MC systems isn't static but susceptible to Brownian motion, the estimation schemes and equalizing algorithm were based on a block-type system. Numerical results in terms of MSE and Cramér-Rao(CRB) show that their equalization method successfully figures ISI and ILI(Inter link interference), and the channel estimation scheme has an improved upper bound performance.

Although there are significant differences between MC and wireless systems, the same idea of achieving a minimum CRB can be applied for both of them in terms of estimation MSE. Furthermore, for Judging the similarity of the systems in terms of heavy traffic and data collision, an assessment, equalization and detection scheme identical but optimal for the wireless system can also be proposed.

Feng M and Jin H proposed (Feng & Hong 2020) an improved algorithm based on DFT that enhances channel estimation in OFDM systems by accounting for both noises outside the cyclic prefix (CP) and inside CP. Their study reveals that most of the data symbols of the OFDM signal are concentrated around the peak amplitude of the time domain signal, and the other components can be considered as noise or irrelevant. As such, their improved DFT scheme used statistical median inside and outside the CP to effectively cancel out the remaining noise even after the LS algorithm. Furthermore, the DFT algorithm is easy to apply, and the BER performance gain was clear after the modification. Finally, they demonstrated the performance of their algorithm against conventional DFT and LS via the BER calculation and the MSE.

However, their results can be further generalized if the number of multipath components is increased. There is generally larger multipath in practical Massive

MIMO scenarios, especially in dynamic situations. Also, accounting for the quality of available channel statistics, an estimate for the MMSE can be extended.

Apart from the Compressed Sensing (CS) algorithms which exploit the sparsity of the spatially correlated MMIMO channels, authors Yilmaz & Erdogan (2019) proposed a Compressed Training based Semi-blind algorithm for channel estimation that doesn't rely on the sparsity of the MMIMO channels. So, it's equally applicable to both sparse and dense channels. The authors exploited the channel reciprocity in TDD MMIMO systems to significantly reduce the training length from the no of users = k symbols to log2k symbols utilizing the uplink pilot section and the uplink data section. Their scheme involves presenting the LS estimate as a convex cost function problem and finding the infinity norm or l ∞ norm of the whole packet. According to the authors, instead of finding the estimate of the channel matrix *H*, finding the linear equalization explicitly using both data and training sessions yielded a better result. They argued that non-convex cost function-based adaptive algorithms suffer from inaccuracies due to undesired minima and slow convergence issues resulting from undesired saddle points.

Nevertheless, presenting the estimation error as a convex cost function has limits on itself as although it's not an NP hard problem to solve, still in the case of multi-user MMIMO the calculation complexity Amelunxen, Lotz, McCoy, & Tropp, (2014) will exponentially rise especially in FDD systems. A comparative analysis of the above literature is given below for clarity-

Table 2-2 Features and limitations of mentioned research works

Article	**Methodology**	**Features**	**Limitations**	**Remark**
(Pan et al., 2019)	FDD Massive MIMO	Efficient separate ML decoding. Easy account of joint decoding performance for	It can be extended to the LS algorithm also.	It shows the combined efficiency when both the detection and

		complex MIMO systems		estimation are considered.
(Singh, Mishra, Jagannatham, & Vasudevan, 2019a)	FBMC-MIMO	The use of sharp FT filters makes CP redundant. Account for statistical info of data symbols further improves the estimation performance	Doesn't account for the channel reciprocity in the case of TDD systems. The SVD operations and the exploitation of statistical info result in far higher computational complexity than the LS method.	The availability of channel statistics becomes crucial in the overall complexity of the algorithm.
(Kuai et al., 2019)	Massive MIMO; GSM	Exploiting clustered channel sparsity and inherent sparsity in GSM significantly reduces pilot overhead. Proposed Blind estimation method reaches Genie-	The performance of the proposed blind algorithms depends on the availability of perfect	Spatial modulations offer some significant advantages over conventional modulations, such as reduced power consumption, redundancy of

		aided algorithm performance The Semi-blind algorithm performs best under short-pilot transmissions.	CSI at the transceiver. Bilinear recovery algorithm is not applicable due to scheme constraints.	antenna synchronization and inter-antenna interference (IAI).
(W. Wang et al., 2019)	TDD Massive MIMO	A two-step channel estimation process protects the system from unauthorized access. Using Eigen Value Decomposition(EVD), contaminated symbols are automatically detected and removed from circulation. MMSE precoding scheme allows us to determine the lower bound on the achievable downlink secrecy maximization.	Channel reciprocity is required as a prerequisite, so only applicable to TDD systems. Applicable for only single-cell scenarios.	Physical layer security can be a major concern for the current 5G era since denser and denser cell structures are being employed in operation.

(Rouzegar & Spagnolini, 2017)	Diffusive MIMO (DMIMO)	Accounts for multi-entities within the system Uses conventional low-complexity pilot training algorithms.	A separate Interleaving encoder is required to exploit the time diversity. The tradeoff of complexity for 1dB gain over the ML and LS methods isn't significant.	The effect of inter-link interference (ILI) in DMIMO is very significant and plays a key role in determining the performance of the channel impulse response (CIR) estimation schemes.
(Feng & Hong, 2020)	Massive MIMO	The low complexity of the proposed DFT algorithm. Doesn't require any channel statistics. Doesn't rely on channel reciprocity.	In denser urban areas, the algorithm must be extended to account for larger multipath components. It can be further enhanced if channel statistics are	Although acquiring channel statistics adds to the overhead, an efficient feedback system can reduce this burden to a certain extent.

			taken into account.	
(Yilmaz & Erdogan, 2019)	TDD Massive MIMO	Proposed algorithm free from slow convergence problems caused by the existence of saddle points. The cost function minimization problem has lower complexity compared to contemporary algorithms. Significantly reduces the required training length.	Algorithm complexity eventually rises in FDD systems.	Convexity of the l_1 and l_∞ minimization problems is becoming popular due to the emergence of CS-based methods. The authors thus also provide a linkage between these two methods.

2.4 BENCHMARKING

For initial benchmarking purposes, we're taking the study of Pan et al. (2019), which provides a good starting point for our optimization since the algorithm studied here is suitable for general FDD Massive MIMO systems. Also, because it's efficient for MMIMO systems to be characterized by the combined performance of decoding and estimation, note that at any stage of this research, if deemed necessary, we're willing to adopt or change our benchmarking parameters, which only time will say.

2.5 CHAPTER SUMMARY

This chapter discusses some of the numerous contemporary contributions in channel estimation and signal processing, from which this study is inspired. Different researchers have tried to exploit different aspects of the MMIMO systems to achieve the same goal, improving the quality and robustness of conventional and contemporary channel estimation algorithms. Furthermore, because the communication in mmWave will have some crucial problems, as indicated in the literature, an efficient CSI-acquiring structure will go a long way in incorporating the signal processing standards of LTE into 5G NR and future releases.

CHAPTER THREE

METHODOLOGY

3.1 INTRODUCTION

Channel estimation techniques can be broadly categorised into Blind, Semi-blind and Training based. Since we're focusing on training-based estimation schemes, the algorithms and methodology from hereon will be about this regime. In the field of pilot-aided training, various approaches can be taken. Some researchers have opted for a soft estimate of data symbols via a max-a-posterior (MAP) decoder to reduce iteration error subsequently (Hardjawana et al., 2010). A vital feature of this scheme is the joint cancellation of ICI from the subcarriers. Including the Doppler spread information at the receiver also shows good performance lower bound on some systems (Aboutorab, Hardjawana, & Vucetic, 2013). The Doppler spread information becomes very useful in high mobility scenarios. The Adaptiveness of the estimator is a very attractive feature that allows the receiver to update the estimator parameters without channel and noise statistics, significantly reducing the calculation complexity (Masud & Kamal, 2010). Although channel and noise statistics can substantially minimize the iteration errors, but also exponentially adds to the complexity. Linear MMSE or LMMSE has superior performance over LS when the considered SNR is small and not rapidly changing, but in varying SNR regions, it loses efficiency to LS (Khlifi & Bouallegue, 2011). Using a minimal degree of channel statistics can yield about ~10% improvement in max throughput and spectral efficiency if the estimation algorithms have decision-directed iteration steps (Ketonen et al., 2015).

By exploiting the null-subcarriers and adding compensation for each iteration process, the traditional MMSE algorithm can produce more accurate CSI with reduced complexity (Y. Liu & Sezginer, 2012).

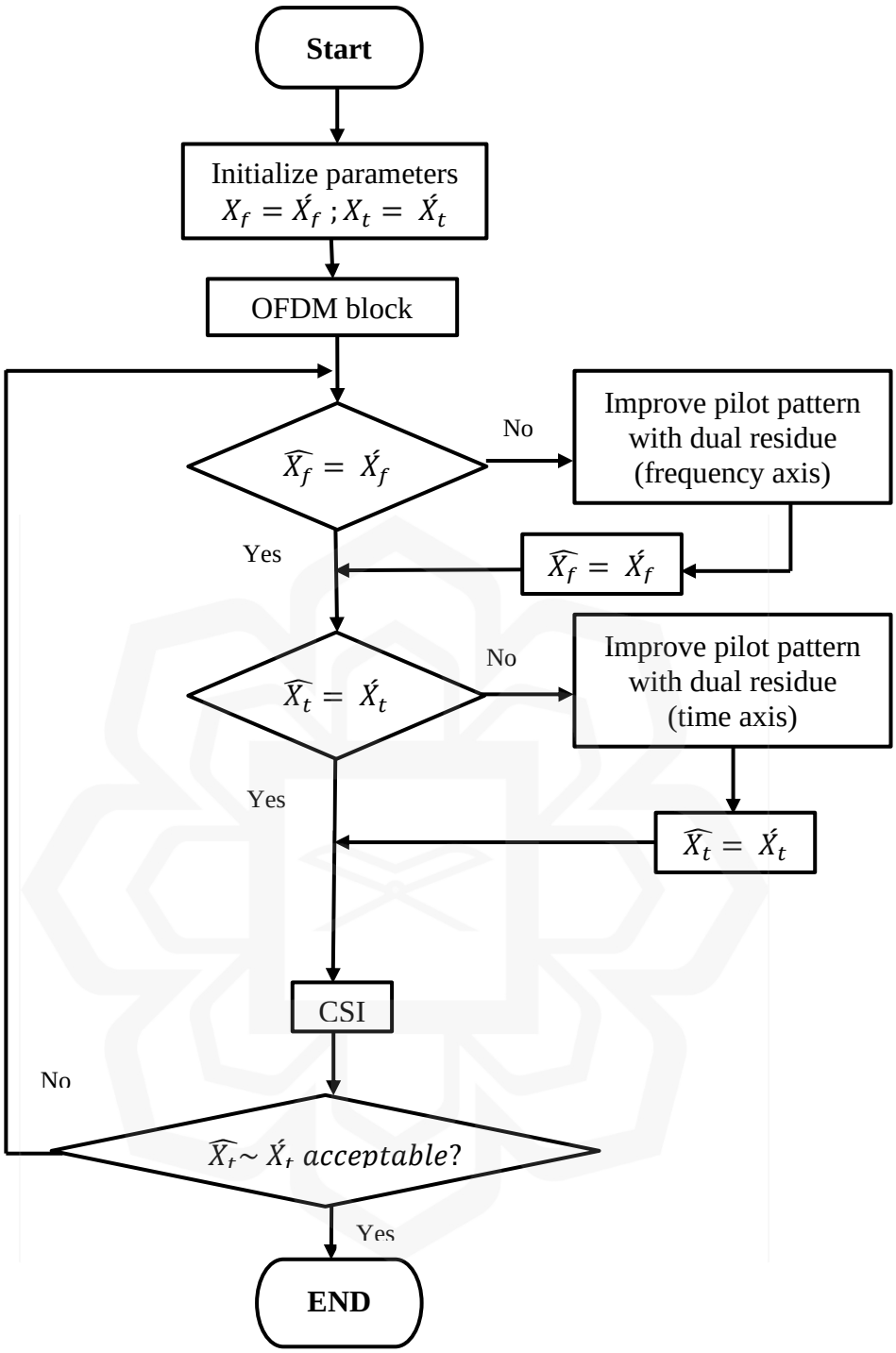

Figure 3.1 Estimator workflow

In light of these approaches, we'll take an adaptive iteration approach that shows significant performance without the added complexity of channel statistics. Another key feature of this approach is that it can be extended to most other algorithms and thus enhance their performance.

As a final remark, the hypothesis of this research can be put into a workflow as depicted in Figure 3.1.

3.2 SYSTEM MODEL

For this study, we're considering a flat block-fading Massive MIMO system with *t, r* – as the no of *Tx* and *Rx* antennas. A block-fading system means that the fading can be assumed constant during the transmission of one symbol. In the frequency domain, we can express the received signal vector as,

$$\boldsymbol{y}_i = \boldsymbol{H}\boldsymbol{p}_i + \boldsymbol{z}_i \tag{3.1}$$

Where, *H* is the $r \times t$ random channel matrix, z_i is the $r \times t$ complex Gaussian noise with zero means, and pi is the $t \times 1$ complex vector of the transmitted signal. For simplicity reasons, we treat *H* as random and its elements as independent and identically distributed (IID). Hence, during the estimation process, any estimate of *H* at a certain time instant will mean a particular sample of this random matrix that pertains to the current block in consideration. For the estimation of *H,* let's assume $n \geq t$ training vectors p1, p2.....pn to be transmitted, now the related $r \times n$ matrix of the received signal *Y* = [*y1, y2.....yn*] can be defined as,

$$\mathbf{Y} = \mathbf{HP} + \mathbf{Z} \tag{3.2}$$

Assuming *N* subcarriers, the symbols for the training matrix *P* can be described as-

$$\boldsymbol{P} = \begin{bmatrix} P[0] & 0 & \cdots & 0 \\ 0 & P[1] & \cdots & \vdots \\ \vdots & \cdots & P[2] & 0 \\ 0 & \cdots & 0 & P[N-1] \end{bmatrix} \tag{3.3a}$$

Where, *P*[k] denotes the pilot at the kth subcarrier. The mean and variance of this pilot matrix are 0 and σ_x^2- respectively, with *k = 0, 1, 2……N-1*. Since *P* is a diagonal matrix, we assume all the subcarriers are orthogonal, i.e., ICI-free. Since we know the channel gain = *H*[k] (impulse response in the time domain) for each subcarrier, the received signal matrix can then be defined in equation (3.3),

$$Y \approx \begin{bmatrix} Y[0] \\ Y[1] \\ \vdots \\ Y[N-1] \end{bmatrix} = \begin{bmatrix} P[0] & 0 & \cdots & 0 \\ 0 & P[1] & \cdots & \vdots \\ \vdots & \cdots & P[2] & 0 \\ 0 & \cdots & 0 & P[N-1] \end{bmatrix} \begin{bmatrix} H[0] \\ H[1] \\ \vdots \\ H[N-1] \end{bmatrix} + \begin{bmatrix} Z[0] \\ Z[1] \\ \vdots \\ Z[N-1] \end{bmatrix} \quad (3.3a)$$

$$= PH + Z \quad (3.3b)$$

where the channel vector H is given by – H= [H[0], H[1]…….H[N-1]] T and Z is the Gaussian noise vector Z = [Z[0], Z[1]……..Z[N-1]] T with mean = 0 and variance = σ_z^2. For the estimation algorithms, we denote H ^as the estimate of H.

3.3 LEAST SQUARES CHANNEL ESTIMATOR

The idea behind the least squares channel estimator is to determine H ^in such a way as to minimize the cost function-

$$J(\hat{H}) = \|Y - P\hat{H}\|^2 \quad (3.4a)$$

$$= (Y - P\hat{H})^H(Y - P\hat{H}) \quad (3.4b)$$

$$= Y^HY - Y^HP\hat{H} - \hat{H}^HP^HY + \hat{H}^H P^H P\hat{H} \quad (3.4)$$

Now by setting its derivative concerning H ^ to zero, we get

$$\frac{\partial J(\hat{H})}{J\hat{H}} = -2(P^HY)^* + 2(P^HP\hat{H})^* = 0 \quad (3.5)$$

Having PHPH ^= PHY solves for the LS estimate of H ^ as-

$$H_{LS}^{\wedge} = (P^HP)^{-1}P^HY = P^{-1}Y \quad (3.6)$$

Let's denote the components of the channel estimate matrix as (H_LS) ^[k]. Where k = 0, 1, 2…..N-1. Since we assumed that P is diagonal, then we can write the channel estimate for each subcarrier as-

$$\hat{H_{LS}}[k] = \frac{Y[k]}{P[k]} \tag{3.7}$$

The mean square error (MSE) of LS estimation can be found as

$$\begin{aligned} MSE_{LS} &= E\{(H- \hat{H_{LS}})^H(H- H_{LS})\} && (3.8a)\\ &= E\{(H-P^{-1}Y)^H(H-P^{-1}Y)\}) && (3.8b)\\ &= E\{(P^{-1}Z)^H(P^{-1}Z)\} && (3.8c)\\ &= E\{Z^H(PP^H)^{-1}Z\} && (3.8d)\\ &= \frac{\sigma_z^2}{\sigma_x^2} && (3.8) \end{aligned}$$

Notice that the system SNR is inversely related to the MSE of the *LS* algorithm. It's because, mathematically, the MSE is the average of the unit square error, which in the case of *LS*, translates into the ratio of AWGN and signal power in the frequency domain. The chief advantage of the *LS* algorithm is it's simplicity in application since no channel statistics or Priori information is required here. The algorithm model in that region shows that the redundancy check step at the end of the conventional algorithm only adds a negligible amount of distance improvement when MMIMO-OFDM scenery is considered. Besides that, it greatly affects the total pilot overhead, as seen from the algorithm steps. If we increase the total number of subcarriers to facilitate the increase in cell users, the pilot overhead will exponentially increase. To accomplish this, the *BS* transmitter has to be adapted to emit an increased number of signal blocks per unit of time.

The proposed method exploits these tradeoffs to offer a better. A recent study (Pan et al., 2019) also showed that evaluating the channel estimation and decoding performance together could enable a good overview of the overall *BER* performance of the OFDM system. The authors demonstrated the performance of joint ML (Max Likelihood) decoding, conventional mismatched ML decoding and a novel scheme that they call separate ML decoding, and the addition of MMSE channel estimation. They used two modulation schemes, 16QAM and QPSK, to show the performance overview. They mathematically proved that these two detection schemes are identical in terms of performance, although conventionally, it has been thought that joint detection schemes are superior. The account estimation error in the separate

decoding scheme is a possible reason. They also showed that MMSE algorithms have the best performance in terms of overall system efficiency. In our methodology, we demonstrated that the cutoff from the checking portion of the algorithm has less effect on performance and more effect on the system overhead. Recent studies also showed that the effect of the numbers of subcarriers gets significant with an increasing no of users. And this has a negative effect on the CE algorithm.

3.4 ESTIMATOR ACCURACY CONSIDERATIONS

As can be guessed from the characteristics of estimators, their accuracy largely depends on the observed sample and the pertaining PDF of that data. As discussed below, we will see that the estimator's accuracy can be substantially effected depending on the degree of correlation of the PDF with the data in question.

3.4.1 Dependency of the PDF on the channel co-efficient

If we treat a single sample of the transmission as-

$$y[0] = h + z[0] \tag{3.9}$$

Where, *y* is the received bits, *h* is the unknown channel coefficient and *z* is the random Gaussian noise.

Where, the AWGN z[0]~(0,σ2) and we want to estimate h, we can speculate that the variance σ2 will be smaller for a better estimate. From the definition of unbiased estimators, we can recall that for the best-unbiased estimation $\hat{h} = y[0]$. From this, it's apparent that the estimator's accuracy increases as the variance decreases. Since we are considering AWGN, the probability density function (PDF) pa(y, h) of the unknown channel parameter can be defined as,

$$p_a(y[0];h) = \frac{1}{\sqrt{2\pi\sigma_a^2}} e^{[-\frac{1}{2\sigma_a^2}(y[0]-h)^2]} \tag{3.10}$$

When we consider the PDF as a function of the unknown parameter h for a certain *y*[n], we can term it as the likelihood function. The acuteness of this likelihood function will show how accurately we can estimate our unknown parameter using our proposed optimized legacy algorithms. The sharpness is usually calculated as the negative of the 2nd derivative of the logarithm of the likelihood function at its max. It's referred to as the curvature of the logarithmic-likelihood function. For instance, consider the log-likelihood function of Equation (3.8) as,

$$ln\, p(y[0];h) = -ln\sqrt{2\pi\sigma^2} - \frac{1}{2\sigma^2}(y[0]-h)^2 \tag{3.11}$$

Where, the σ^2 is the variance of the random Gaussian noise.
The 1st derivative is-

$$\frac{\partial\, ln\, p(y[0];h)}{\partial h} = \frac{1}{\sigma^2}(y[0]-h) \tag{3.11}$$

So we can calculate the negative of the 2nd derivative as-

$$-\frac{\partial^2\, ln\, p(y[0];h)}{\partial h^2} = \frac{1}{\sigma^2} \tag{3.12}$$

Apparently, the curvature is inversely proportional to σ2, which in this case is the variance. So for our case, we can write from equation (2.10),

$$-\frac{\partial h^2}{\partial^2\, ln\, p(y[0];h)} = var(\hat{h}) \tag{3.13}$$

Where, var(hˆ) indicates the variance of the unknown channel coefficient *h* to be estimated.

In the proposed wireless channel estimation model, the wireless channel Co-efficient will certainly depend on the value of y[0] since we know that the covariance matrices are highly correlated in MIMO-OFDM systems. So to put it more precisely, we can present equation (2.11) more compactly. So the expectancy or the average of the lower bound will be,

$$-E\left[\frac{\partial^2 \ln p(y[0];h)}{\partial h^2}\right] = Curvature \tag{3.14}$$

Equation (2.12) measures the average curvature of the log-likelihood function. As we can see, the expectation or mean is taken with respect to p(y[0]; h), turning it into a sole h-dependent function. From equation (2.12), we can guess a couple of intuitive assumptions. For instance, the likelihood function, which depends on y[0], is a random variable. Also, the larger the curvature of the likelihood function, the smaller the variance of the unknown parameter h.

3.4.2 The Cramer-Rao Lower Bound Delimitation

We shall also derive the Cramer-Rao lower bounds for our scenario, which is a very common and effective way to judge the accuracy of the estimation process and its deviation from the actual value of the parameter. For our case, we can indicate the received signal vector as a function dependent on the unknown parameter h, which we wish to estimate via the algorithm-

$$y[n] = x[n;h] + z[n] \tag{3.15}$$

Where, y is the received bits, x is the transmitted bits, and z is the random noise matrix.

We can explicitly note the dependence on the received signal vector on h. From equation (3.15), we can define the likelihood function p(y; h) as,

$$p(y;h) = \frac{1}{\sqrt[N]{2\pi\sigma^2}} e^{\left[-\frac{1}{2\sigma^2}\sum_{n=0}^{N-1}(y[n]-x[n;h])^2\right]} \tag{3.16a}$$

Through differentiating once we get-

$$\frac{\partial \ln p(y;h)}{\partial h} = \frac{1}{\sigma^2}\sum_{n=0}^{N-1}(y[n]-x[n;h])\frac{\partial x[n;h]}{\partial h} \quad (3.16b)$$

Differentiating for the second time results in-

$$\frac{\partial^2 \ln p(y;h)}{\partial h^2} = \frac{1}{\sigma^2}\sum_{n=0}^{N-1}\left\{(y[n]-x[n;h])\frac{\partial^2 x[n;h]}{\partial h^2} - \left(\frac{\partial x[n;h]}{\partial h}\right)^2\right\} \quad (3.16c)$$

Now we take the expected value as-

$$E\left(\frac{\partial^2 \ln p(y;h)}{\partial h^2}\right) = -\frac{1}{\sigma^2}\sum_{n=0}^{N-1}\left(\frac{\partial x[n;h]}{\partial h}\right)^2 \quad (3.16)$$

So that we can finally state that-

$$var(\hat{h}) \geq \frac{\sigma^2}{\sum_{n=0}^{N-1}\left(\frac{\partial x[n;h]}{\partial h}\right)^2} \quad (3.17)$$

The degree of dependence of the transmitted signal is demonstrated by this bound. From equation (3.16), we can say that signals sensitive to small changes in the unknown parameter h result in better estimation performance. It should also be noted here that any nonlinear transformation of the signal space will result in a rapid declination of the estimator's accuracy. It is because any non-linear transformation transfers the estimator from the unbiased domain to the biased domain. So as long as the linearity of the CRLB is maintained, we can expect an unbiased estimate of the unknown parameter.

We can now take a look at how the algorithm looks according to the discussion so far,

Input: $\bar{x}$,$\bar{y}$,$\bar{z}$

Output: $\hat{\imath}$ for j attempts

Initialization: set residual $r_0 = \bar{y}$; $\hat{\imath} = 0$; $h = s$; $j = 1$; stage = 1

while $\neq$ $(\|r\|_2 < \|r_{j-1}\|_2)$

Step 1: ***Start;*** Initial select $s_j = max(|i * r_{j-1}, h|)$

Step 2: Create test vector $L_j = \emptyset \cup s_j$

Step 3: Finalize test vector $L = \max\left(\left|i_{L_j}^*\right|, h\right)$

Step 4: Residual $r = \bar{y} - i_L i_L^* \bar{y}$

Step 5: If $\|r\|_2 < \left\|r_{j-1}\right\|_2 \rightarrow step\ 7\ \boldsymbol{else} \rightarrow step\ 4\ ; h = h + 1$

Step 6: Update $L = h \times s$ ***or*** $L_j = L$; $r_j = r$; $j=j+1$

Step 7: $\hat{\imath} = i_L^* \bar{y}$; ***end loop*** ; ***Stop***

After Step 5, where the comparison is done to determine if the current residual factor meets the threshold or not, in Step 7, an intuitive weight adjustment is done where one can see that it adds another layer or offset, which furthers the estimator to the ideal value.

3.5 PHASE ESTIMATION

Theoretically, a phase estimator doesn't exist that attains the CRLB and, at the same time, is unbiased. As a result, it is desirable to look for an MVU estimator instead, which theoretically is still possible to obtain, at least for this case.

An unbiased estimator that attains the CRLB as a sample mean estimator is considered efficient in that it efficiently uses the sample space data. On the other hand, an MVU estimator may or may not be efficient. So it shows that an estimator that doesn't attains the CRLB still be considered an MVU estimator if it's variance is uniformly less than the other estimates. Again, taking the expectancy equation (3.16), the CRLB can even be expressed in a slightly more comfortable form as below; note that all the parameters remain unchanged,

$$E\left[\left(\frac{\partial ln\, p(y;h)}{\partial h^2}\right)^2\right] = \quad -E\left(\frac{\partial^2 ln\, p(y;h)}{\partial h^2}\right) \tag{3.18}$$

Where, the parameters bear the same meaning as in equation (3.17)

So that the variance can be expressed in a more compact form-

$$var(\hat{h}) \quad > \frac{1}{E\left[\left(\frac{\partial ln\, p(y;h)}{\partial h^2}\right)^2\right]} \tag{3.19}$$

The parameter at the denominator on the right side of equation (3.18) is called Fisher information and is defined by-

$$I(h) \quad = -E\left(\frac{\partial^2 ln\, p(y;h)}{\partial h^2}\right) \tag{3.20}$$

It should also be noted here that any nonlinear transformation of the signal space will result in a rapid declination of the estimator's accuracy. It is because any non-linear transformation transfers the estimator from the unbiased domain to the biased domain. So as long as the linearity of the CRLB is maintained, we can expect an unbiased estimate of the unknown parameter. It is one of the reasons CRLB is used unanimously for parameter estimation.

Incorporating the effect on phase, we can further enhance our previous algorithm as follows,

Input: $\bar{x}$, $\bar{y}$, $\bar{z}$

Output: $\hat{h}$ for *k* attempts

Setup: set *residual* $r_0 = \hat{y}$; $\hat{\imath} = 0$; $i=s$; $j = 1$; *attempt = 1*

while $\neq$ ($r_a > r_b$)

Step 1: ***Start ;*** select $f_j = max\left(\left|i * r_{j-1}, h\right|\right)$

Step 2: Create test vector- $L_j = \emptyset \cup s_j$

Step 3: Finalize test vector $L = \max\left(\left|i^*_{L_j}\right|, h\right)$

Step 4: Residual $\boldsymbol{r_a} = \bar{y} - i_L i^* \bar{y}$ *; Resudual* $\boldsymbol{r_b} = \bar{y} - h_L h_L{}^* \bar{y}^*$

Step 5: Check $\boldsymbol{r_a} \sim \boldsymbol{r_b}$; $\boldsymbol{r_a} > \boldsymbol{r_b} \rightarrow$ step 6 ***else*** $\rightarrow$ step 2 : $\hat{\imath} = \hat{\imath}^* f_j(\hat{h})$

Step 6: If $\|r\|_2 < \left\|r_{j-1}\right\|_2 \rightarrow step\ 7$ ***else*** $\rightarrow step\ 4 ; h = h + 1$

Step 7: Update $L = i \times f$ ***or*** $L_j = L$; $r_j = r$; $j = j+1$

Step 8: $\hat{h} = \frac{h^*{}_L}{r_a{}^* \; r_b}$; ***end loop***

Stop

As can be seen, incorporating a dual residue factor instead of one can further improve the estimation by allowing a two-step justification process.

3.6 SPARSITY BASED ESTIMATION

In recent years it's become somewhat of a trend to exploit the sparsity of uncompressed signals. Technically, most natural signals are sparse, meaning signals that haven't yet gone under compression or another kind of processing. Sparse means that some domain must exist where most of the components of that signal can be rendered zero. Therefore that signal can be reconstructed using samples much less than that depicted by Nyquist in his famous formula. Compressed or compressive sensing is one of the most popular schemes currently exploiting the sparsity of natural signals like the image. Compressed sensing is comprised of three major steps: sparse approximation, sparse representation and sparse reconstruction. One thing that should be noted for compressed sensing is that although compressed sensing is based on a fairly old statistical theory, its application to signal to process hasn't seen the light in the past ten years. The main reason behind this is that each step in compressed sensing requires enormous calculation power that wasn't possible until recently. Now in the age of powerful AI-based supercomputers are more than capable of dealing with these kinds of calculations. If the appropriate type of reconstruction is used, the performance upper bound of compressed sensing is immense, leading to its popularity in signal processing. One of the objectives of this research is to compare the performance of the optimized methods with the compressed sensing estimation. Since because of superior performance, compressed sensing algorithms are taken as a benchmark on the performance side, while on the resource allocation side, it has a hefty effect.

3.7 RESEARCH PARADIGM

For this thesis work, we are focusing on developing our model for acquiring channel state information or CSI based on pilot training-based channel estimators like LS, MMSE, LMMSE etc. However, the cost of the equipment for transmission in the EHF band, our research work is limited to simulations via only Matlab simulation. It's

intended to benchmark against existing models and demonstrate the performance upper hand without the use of highly constraint-based algorithms. Having said that, these simulations will include results based on SER, BER, MSE and or other criteria if possible.

3.8 CHAPTER SUMMARY

In this chapter, the foundation for the adaptive algorithm has been laid. It was shown that the redundancy present in the conventional estimator could be exploited if used with an adaptive weight factor. Different characteristics affecting the estimator's performance have also been analysed mathematically. The process of parameter estimation and it’s amelioration in the new algorithm has been thoroughly explained. Based on the framework laid in this chapter, the results of the simulations and discussions on that will be carried out in the successive chapters.

CHAPTER FOUR

RESULTS AND DISCUSSIONS

4.1 INTRODUCTION

This chapter includes the simulations of the modified channel estimators and their benchmarking. This work evaluates performance via the most common criterion for estimators such as MSE, SER, BER & PER. It should be noted that this study is only interested in estimating the amplitude and phase shifts of the transmitted symbols and doesn't concern about offsetting or equalization. The equalization of the estimators at the receiver is to be considered as a future study or an extension of this thesis. Also to be noted is that the algorithms used aren't based on Monte Carlo theory; thus, the simulations are generic and not completely unbiased. This is left as another future recommendation for this type of study. All simulations are performed on the Matlab® 2020b platform and thus may slightly differ in appearance from previous works. Also, for the sake of simplicity, we assumed a single-cell MIMO-OFDM system which may be extended to a multi-cell scenario. Although it's not part of this study, a precoding scheme that follows the modified channel estimators can further enhance the throughput of the wireless system. For benchmarking purposes, the conventional estimator is usually given inside the same graph unless there are weighted versions of the same estimator.

4.2 ESTIMATION PERFORMANCE

For the least square estimator, combining it with adaptive weight has positive effects on the estimator convergence. Instead of adding a static weight, the resultant reception gets better if the weight function adapts itself each time a new signal block is received. This was done by splitting the weight function into two residue parameters and redefining it in each estimation as the ratio of their convoluted sum. We can comprehend this from Figure 4.1.

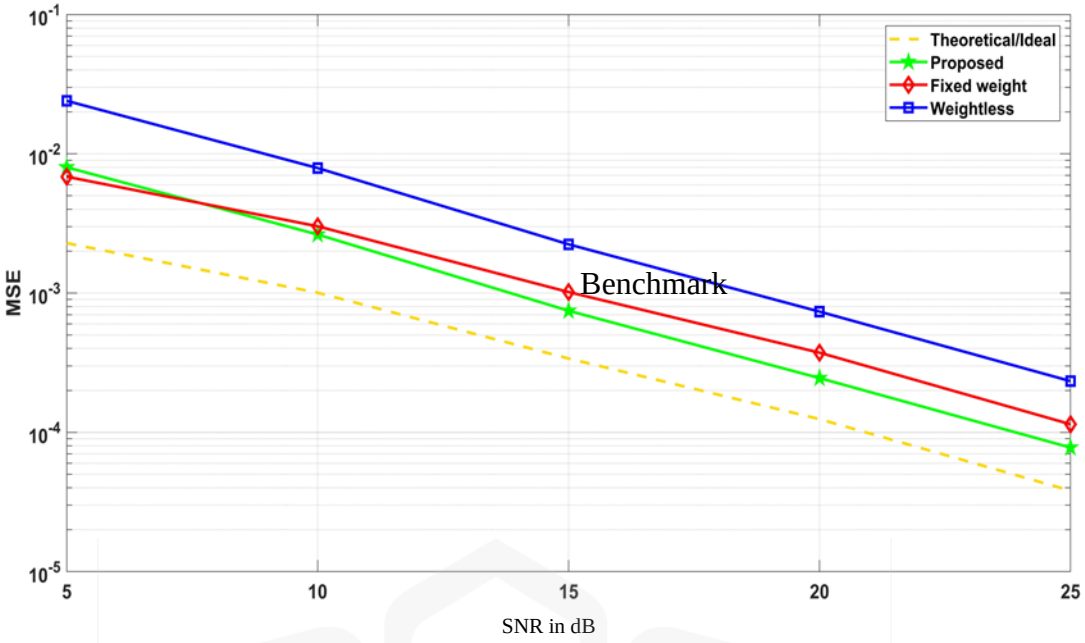

Figure 4.1 MSE comparison.

The BER response follows with a static offset for non-adaptive estimators, as seen in Figure 4.2. The rapid converging curves mean that with increased SNR per bit, the iterations perform better and show faster and less error-prone estimation. It should be mentioned here that the convergence of the curve is also subjected to the channel model adopted, i.e. if there is a LOS path or not. For instance, we adopted a Rayleigh fading for our channels because the NLOS path was chosen for the transmissions. Because the Rician model assumes at least one LOS path, so if a Rician model is used, it may result in a slightly different composition. But the overall response will all be the same as this study's objective is to examine the overall response of the channel estimation performance.

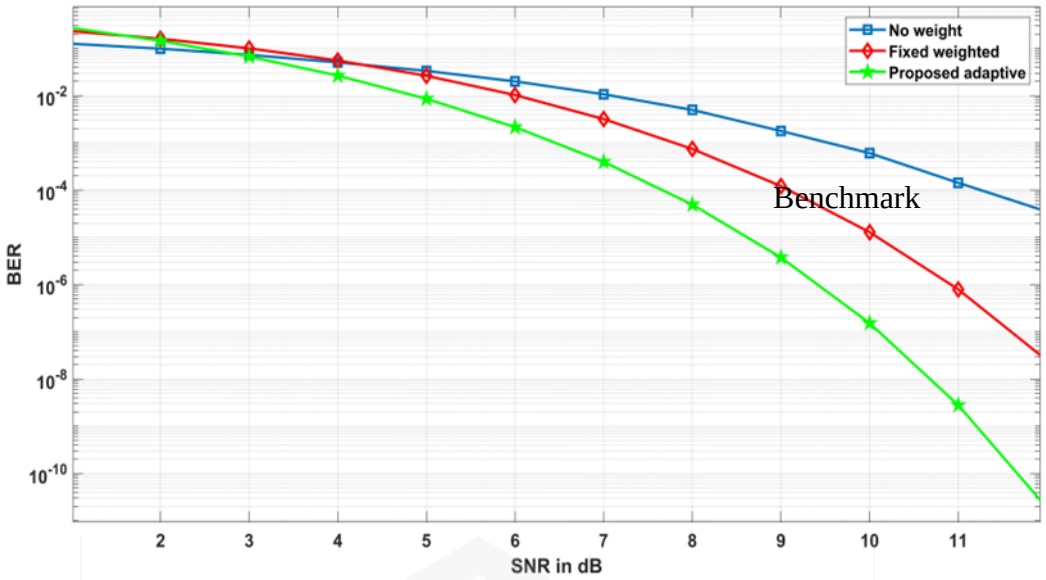

Figure 4.2 BER comparison.

It is to be noted that the dropping nature of the curves in the aforementioned result is natural; that is, it's common for communication systems to have a decreasing BER curve with increasing SNR. Another important reason for decreasing error rates with increasing SNR is the noise floor. The noise floor is the ambient power in the operating RF spectrum and can depend on frequency, location, temperature and bandwidth. Transmitter powers are tuned accordingly to operate well above the noise floor. The important point to note is how the curves act before converging to a negligible value. In that light of information, we can see that the BER curve for our proposed method has a much sharper response compared to the other alternative methods. It has to do with the inherent quality of the algorithm that allows a much smaller margin for errors between successive estimations.

It is interesting to note that the proposed scheme is comparable to the results obtained by the l_1 minimization norm when the sparsity of the signal is exploited

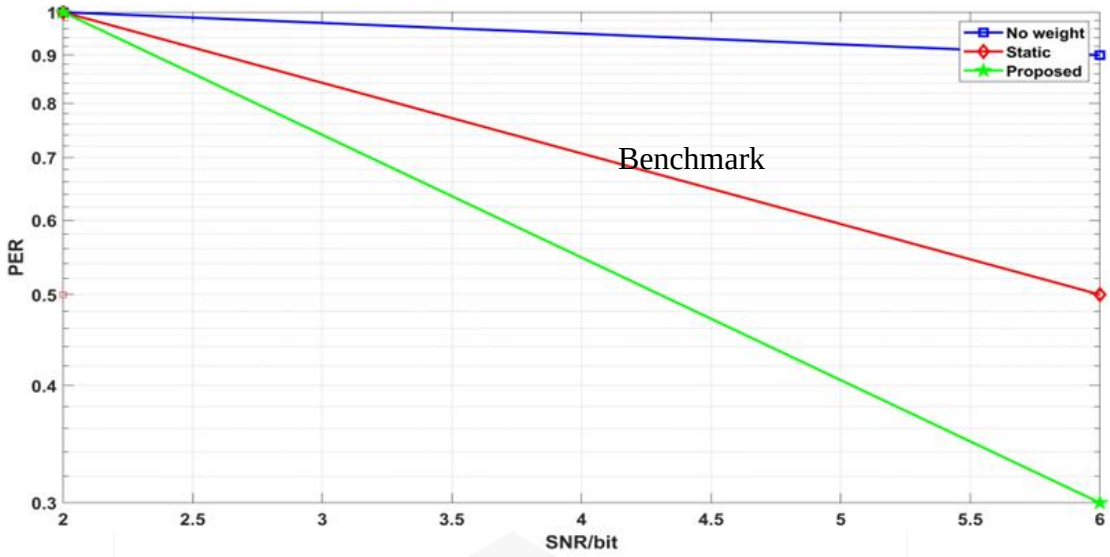

Figure 4.3 Packet error rate comparison.

But since it doesn't require the additional steps necessary for sparse reconstruction, it can be concluded that in terms of system overhead, it will be more resource friendly. A lower packet error rate also measures the T_x efficiency, an important criterion for data and control channels. The figure shows that the higher the system is operated from the noise floor, the better the algorithm performs. As mentioned, there are quite a few elements to incorporate before determining the noise floor for the coverage area. But that analysis is out of the scope of this research and can be taken as a future work instead. The packet error rate curve demonstrates how the data are dealt with after transmission and before reception as a whole.

Since we know that in practical cellular systems, it's impossible to transmit a vast amount of user data continuously, they are sent as packets of information. And that's why it can be somewhat informative to see the system's behaviour as data units or packets. For Figure 4.4, the comparison is made based on the performance of difference l minimization techniques compared to our proposed method. l minimization techniques are popular for their performance upper hand but are difficult to compute. The less the no of minimization, the harder it is to compute usually. So even compared to these techniques, we can see the substantial comparability of our method with the aforementioned ones.

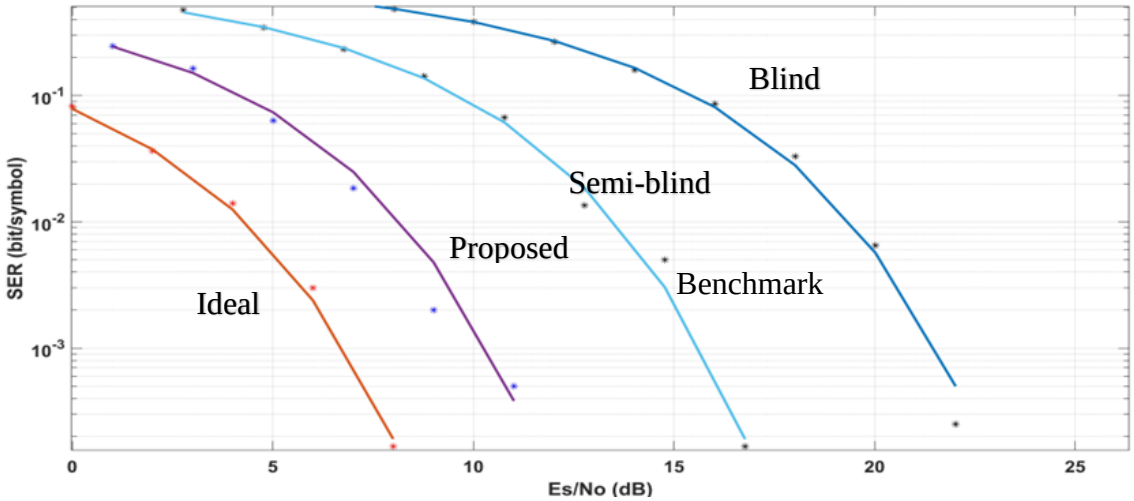

Figure 4.4 Comparison of the proposed scheme with benchmarking schemes.

As for the dispersion of data as packets, we can see from Fig 4.5 that an adaptive scheme lowers the possible data compromise to reduce the overall PER. An overall reduced PER will also mean that the probability of failure of successive packets will be further reduced. It should be noted that a system with filter banks has been used for this simulation, unlike the simulation in Figure 4.3.

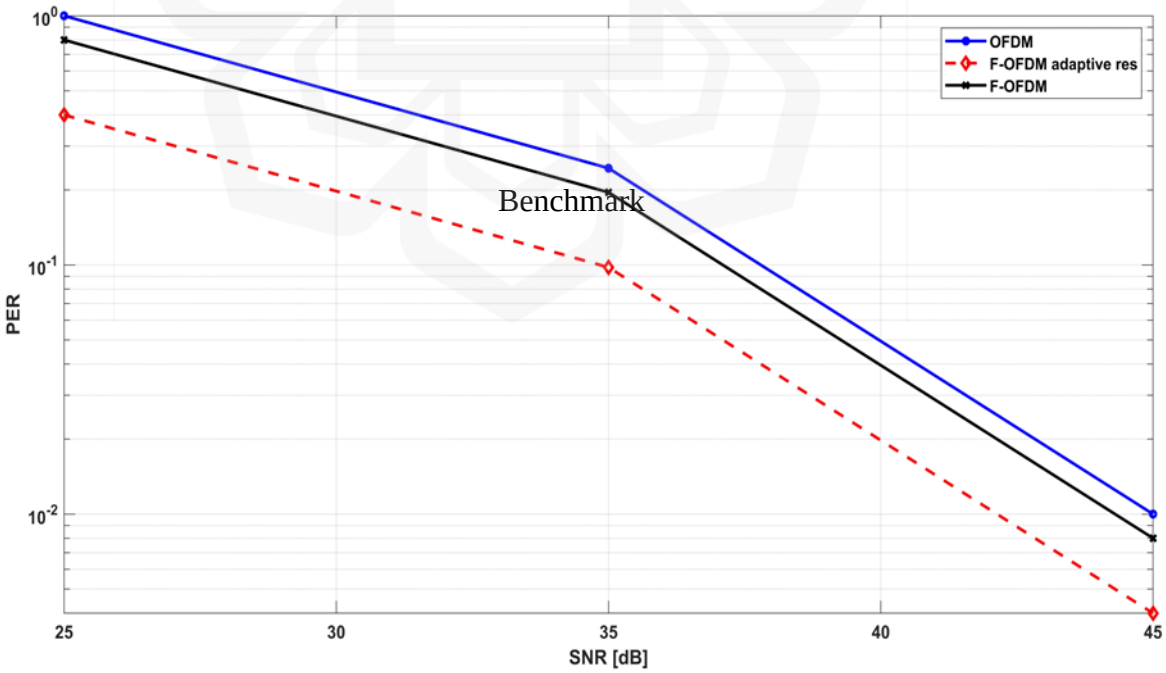

Figure 4.5 Packet error rate comparison of the proposed method

Figure 4.5 also shows that the proposed algorithm can improve the conventional scheme for band-limited systems. It can be seen that the effective operating range for this system starts around 35dB and drops fast ongoing.

In another simulation the benchmark paper using convex optimization was compared to the proposed model. The resulting curves can be seen from the graph below-

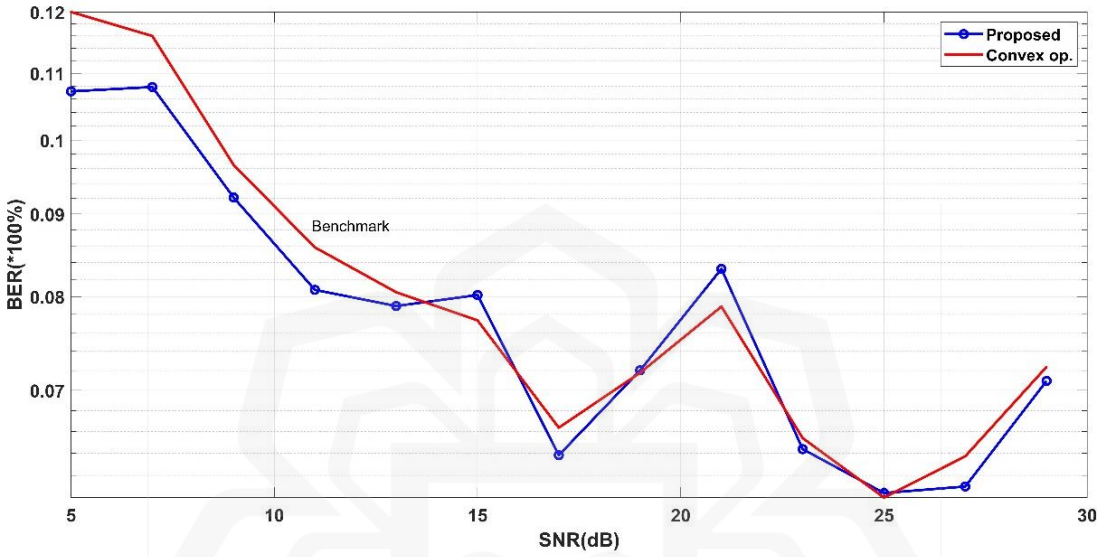

Figure 4.6 Comparison between convex optimized model (benchmark) and proposed model.

As we can see from Figure 4.6 even without using the convex optimization algorithm, the resulting error rates are similar and get's gradually better in higher signal to noise ratios. This is partially due to the absence of additional constraints that adds noise to the base model. Furthermore, in complex systems the additional constraints may add extensive load which will in turn increase the total system overload on the transmitter or the receiver.

Convex optimization may only be used in cases where the error rate at the receiver is too high to be detected. In these cases the no of redundancies have to be increased because the optimization algorithm alone will not be sufficient enough. From the figure below it can also be inferred that if the receiver is planned to work in a specific SNR range then the no of redundancies can be reduced to specifically address that SNR range. Since we are only interested in that specific range the outliers outside that range can be safely ignored without compromising any substantial efficiency. It can also be seen that the proposed model has good SNR in the beforementioned range.

To confirm the validity of the previous simulation , a subcarrier no lower than the standard had been taken. This is to study if the no of subcarrier has any substantial effect on the proposed algorithm compared to the benchark one. The achieved results are shown below:

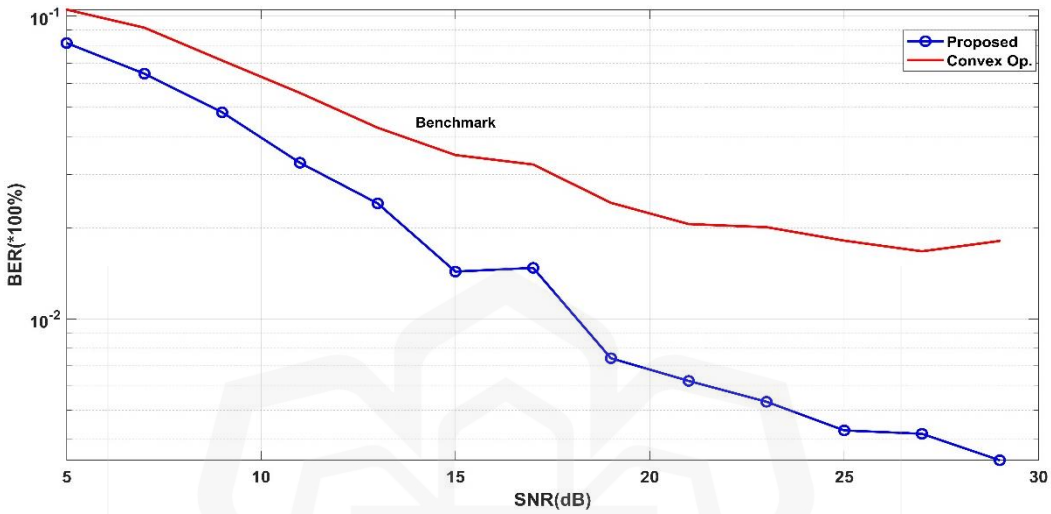

Figure 4.7 Analysis of the proposed model with the convex model in sub-standard scenarios

From Figure 4.7 it can be seen that even in sub-standard scenarios the proposed model work better than the benchmark convex model. And again we see that in higher operating range it gives a much clearer picture of it's efficiency.

Although systems that use <256 subcarriers per channel is not standard and not used commercially these days, in non commercial scenarios like experimental setups this result can be beneficial. Usually in laboratory scenarios where higher frequencies and higher subcarriers per channel may not be viable the proposed algorithm can still perform at an optimal efficiency to yield the best possible error rate per transmission attempt.

One of the reasons that may cause the convex model to have poor performance under sub-par conditions is the algorithm doesn't give substantial error reduction when the no of subcarriers and tap is lower than it's standard values. Here no of taps is also important since it how affects the delay calculation and also the effects of fading. But most importantly, since this simulation is done under sub-standard conditions it will not affect transmission under standard situations where the convex curve will pick up with the increasing no of subcarriers and taps on the channel. What should be inferred from

this graph is that under identical no of taps and subcarriers the proposed model still outperforms the benchmark model.

Another interesting phenomenon can be detected once we double the tap on the channel. Like mentioned above taps are used to calculate delays and affect the ways multipaths are treated. In the next simulation the tap was doubled and it gave a surprising result when compared to the convex optimization algorithm:

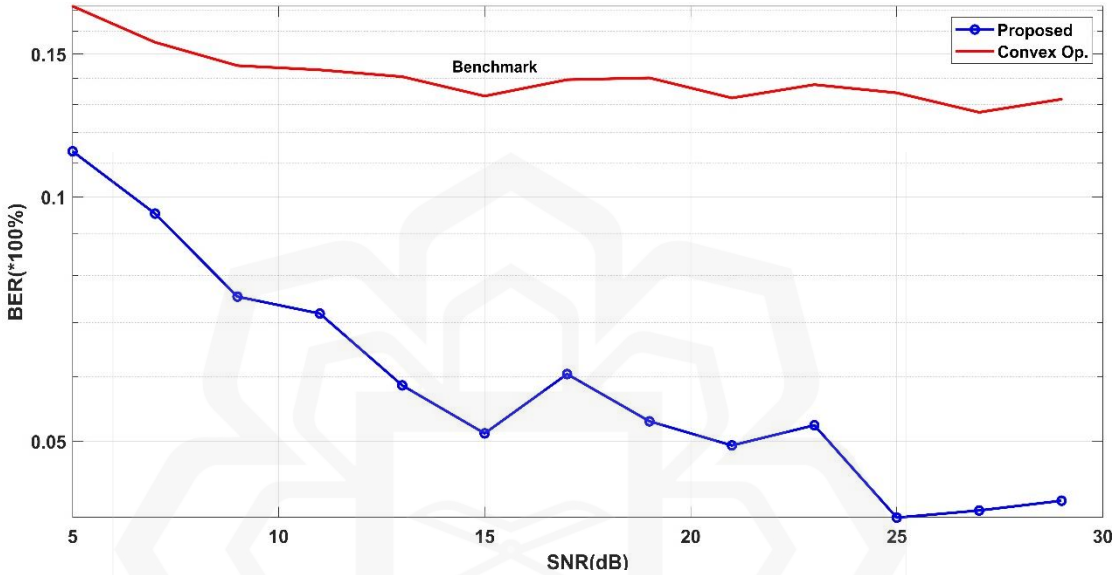

Figure 4.8 Doubled-Tap comparison between benchmark model and proposed algorithm

We can see from Figure 4.8 that doubling the tap no surprisingly flattens both of the curves. Also can be noticed that both of the curves has much less variance compared to when the taps are halved. The convex optimization model is especially affected since it heavily depends on the approximation of the delay at limited intervals. If the taps are increased without increasing the no of subcarriers the resulting curve is flattened since the delays and multipaths have to be calculated and compensated again from the beginning. The proposed curve isn't affected that much since the redundancies are reduced and the weight is made adaptive. Which results in a much stables response. If we see the previous graphs it can be seen that the proposed model is much unaffected compared to the convex model.

And the much reduced variance in both of the curves can be explained from the structure of both of these algorithms. The convex model uses sparse approximation which treats the signal block as basically empty matrix. When a sparse matrix is gone

through delay and other types of attenuation the effects will be very little since most of the elements are zero. And for the proposed model, because the residue weight function is calculated as a mean of the two previous approximation, it also reduces the affect of no of taps.

For the last simulation between the convex optimization model and the proposed model the carrier frequency was chosen as the deciding parameter. All the other parameters were kept constant to see the affect of variance in channel frequency. The resulting graph can be seen below:

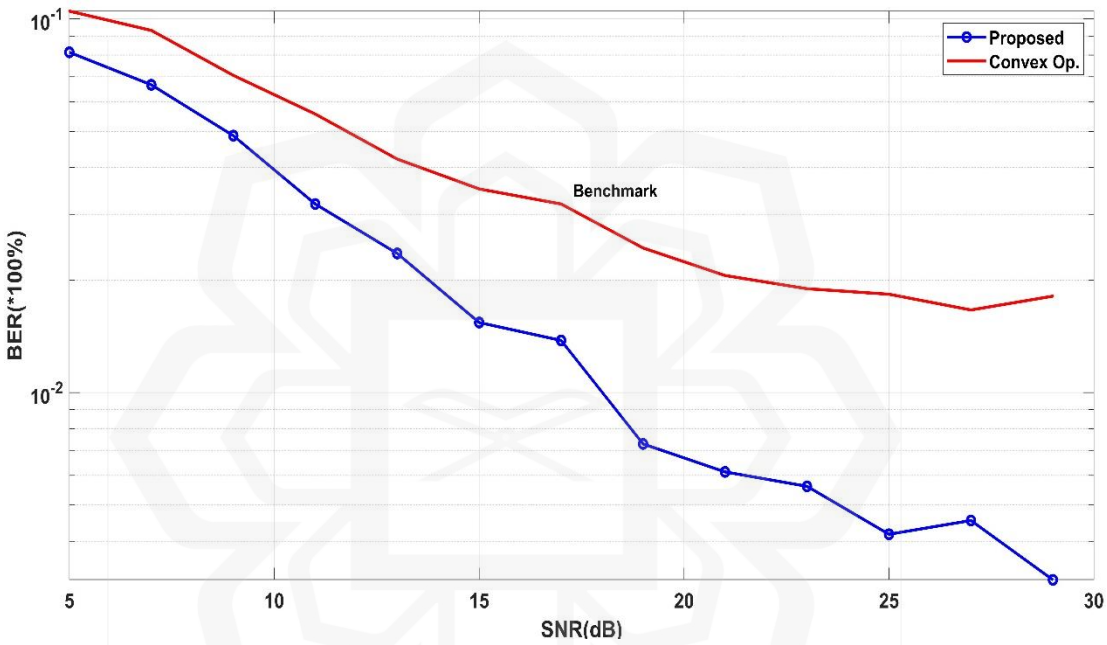

Figure 4.9 Affect of channel frequency change on different models

If we go back to Figure 4.7 we can see that Figure 4.8 is almost identical to it apart from the lower SNR range. Also both of the curves in either cases has a similar kind of response.

This is because in higher SNR especially for the mmWave range the change in doppler frequency has very little effect. This effect can be magnified by employing more subcarriers in a certain channel. It is not included for the sake of minimizing redundancy. However, at higher range after 25dB the difference between the convex model and the proposd model becomes more evident. This is due to the same reason aforementioned, in higher SNR the benchmark model constraints take a heavy toll on the complexity which adds further noise to the overhead. Fortunately most commercial

transmitter and receiver has some offsetting function which compensates some of this added noise generating from a combination of thermal noise and white noise.

In another simulation, a Rician channel model instead of Raleigh one was adopted to see how the change affects the noise profile. It is worthwhile to mention that even though in most cases a Raleigh model fading is adopted because it is considered that no direct line-of-sight is available but in certain cases a Rician profile may be suitable. In the previous simulations the Rayleigh profile was used. The algorithms were adopted then to simulate the effect of a Rician profile which assumes at least one line-of-sight path. The results can be seen from the graph below-

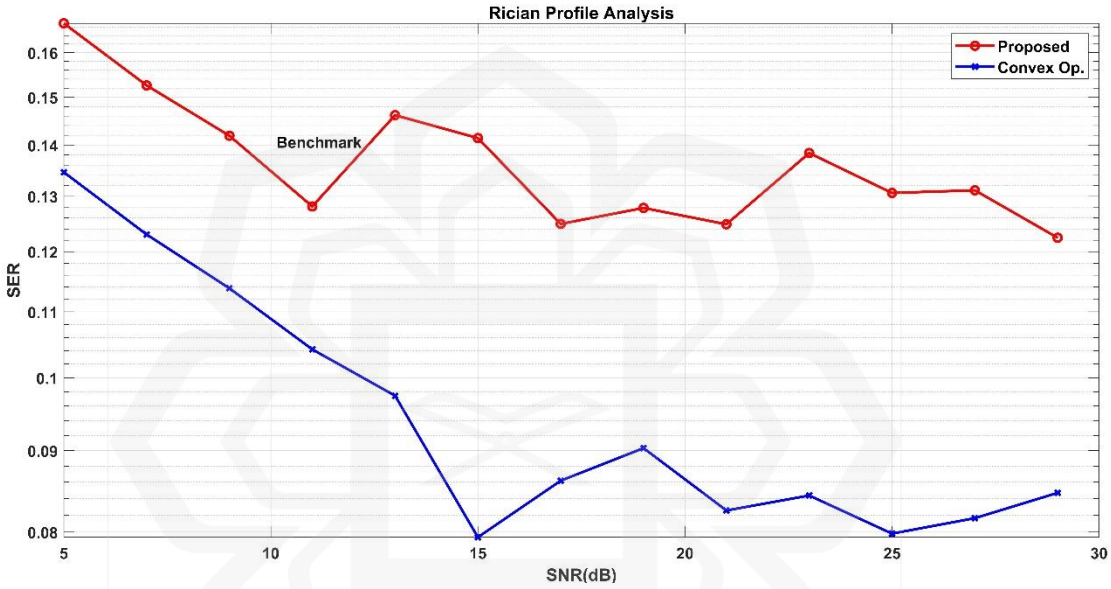

Figure 4.10 Rician profile analysis between the benchmark model and proposed.

It is quite evident from Figure 4.10 that in terms of SER the proposed model shows significant improvement over the convex optimization model. The erratic response of the curves at higher SNR is indicator of adoption of the Rician model which considers phasor sum of several copies of the transmitted signal in the receiver. Like mentioned before this sum has to contain at least one LOS component and the other components can be any delfected signal.

It should be noted that the erratic behavior in Figure 4.10 which appears around ~15dB will continue in even higher SNR ranges. In fact in much higher SNRs than standard operating range the sudden ramping of the signals should increase technically since the thermal noise and other internal noise elements will add up. That is why in commercially operated stations Rician models are almost never adopted and their utility is often times limited to only experimental cases. However it should be mentioned too

that the erratic behavior is proportional to the distance of the transmitter and the receiver in this case since the further they are the higher are the chances that the random components have a higher phase shift.

Another distribution that has caught attention recently is the Weibull model which also has good indoor and outdoor noise floor. To simulate the Weibull model the Monte-Carlo Simulations (MCS) settings have to be used. For that, the MCS built in function in Matlab was adopted. The advantage of the MCS setting is that higher no of trials can be put to more precisely delineate the performance upper bound of the channel model under the proposed algorithm. As with the previous simulations, the proposed model was compared against the convex model as a benchmark and the following results were obtained:

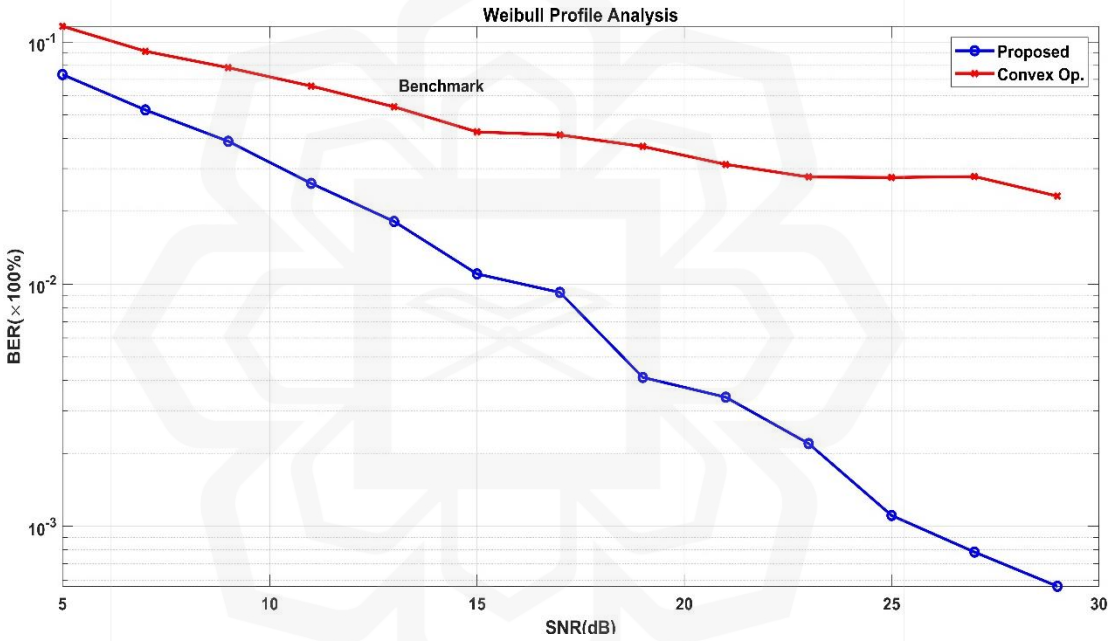

Figure 4.11 Weibull Profile analysis against benchmark.

In Weibull envelope the difference between the proposed and the convex model is much subtler as compared to Figure 4.10. However, this subtle difference is an indicator of the affect of Weibull's probability density function or PDF on the algorithm. Since the PDF of Weibull is of Gaussian type, using the MCS package the distribution function was numerically estimated first. Then the function was incorporated into the proposed algorithm to simulate the effects of a Weibull noise envelope. Nevertheless, despite being in a smaller margin the BER can be still substantially different as is apparent from Figure 4.11. The question may arise as to why industrially this distribution isn't adopted since it evidently has better performance than

other noise envelope. It is because creating the noise profile with MCS is very hardware consuming and in higher trials the system overhead can be extremely high to adopt. Hence like the Rician profile it's usually limited to experimental cases only.

The Nakagami distributions are also a recent trending method of estimating the attenuation margin. To compare the proposed model attenuation using Nakagami distribution the Matlab built-in Chi distribution function was adjusted so that the resulting PDF follows the Nakagami definition of Gamma function. However the Nakagami distribution can also be obtained using the Gamma function itself. But in our case owing to the configuration of the proposed algorithm, it's quite difficult to achieve the satisfactory random variable to generate the distribution. Hence we follow the former mentioned procedure to generate the distribution using Chi functions instead.

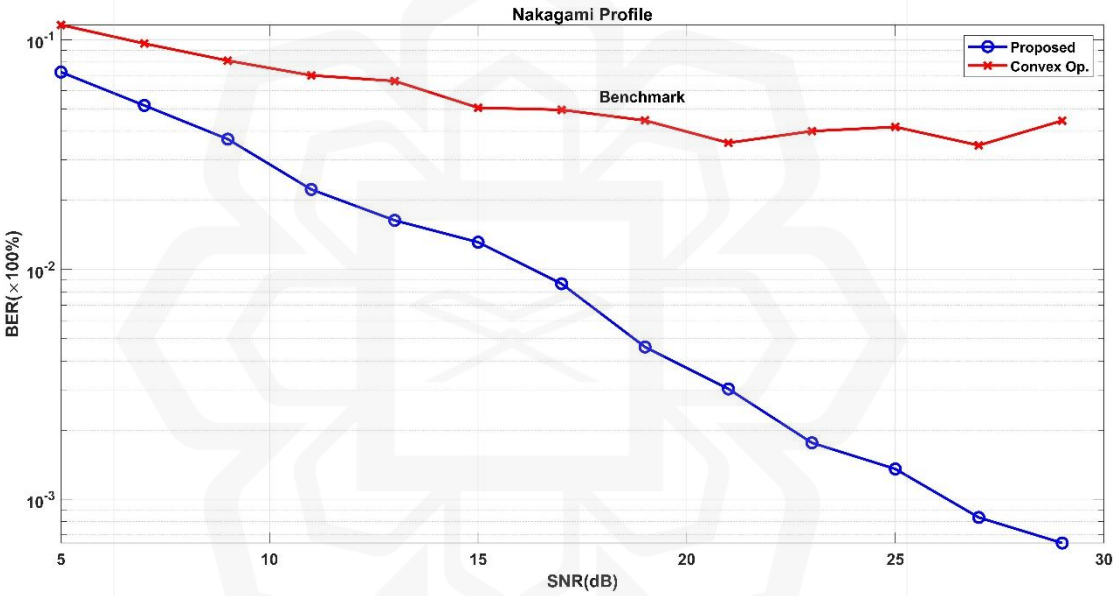

Figure 4.12 Comparison between proposed model and benchmark using Nakagami profile

From the Figure 4.12 it's evident that in terms of error rates and attenuation the Nakagami profile does not differ too much from the Weibull profile. The reason is inherent in the derived PDF in both of these distributions. Weibull fading which is based on the identically named distribution has similar characteristics PDF under certain conditions. The generated random functions can have identical definition in some cases.This is why it is seen that both in the cases of Figure 4.11 and Figure 4.12 the around the ~25dB range the benchmark convex model start deteriorating abruptly especially in the case of Nakagami profile.

As with the case of Weibull model, Nakagami distribution although gaining attention recently but still is not adopted as an industry standard for commercial signal processing and wireless networks. Nevertheless, it's still a useful profile for analysis when there are multiple numbers of multipaths and the resulting signal has to be offset at the receiver.

The point-to-point(p2p) performance of the proposed model can be analysed under two different scenarios. Since we are assuming a frequency selective wireless media in our simulations, it can be simulated in both coherent and noncoherent configuration. The effect of addition of the forward error correction (FEC) to the proposed method can be identified from the two scenarios. First for the coherent simulation, the FEC function is added to the code and the required parameters are passed as the elements. This function is called from inside the code during simulation to simulate a coherent point-to-point OFDM signal.

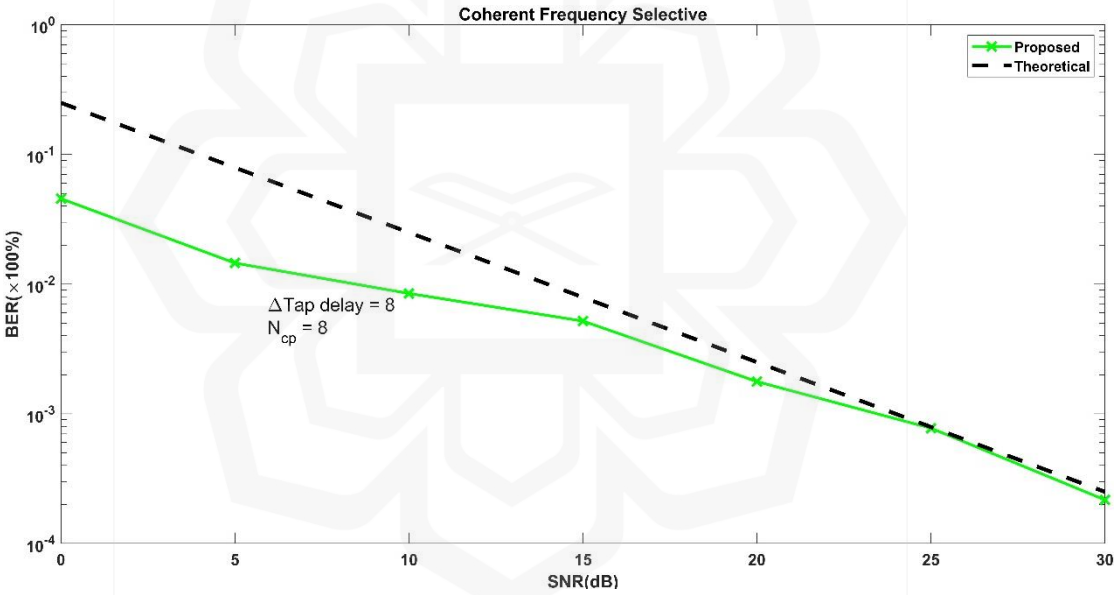

Figure 4.13 Simulation of the proposed algorithm in Coherent p2p configuration.

There are two different curves in the coherent configuration simulation. From Figure 4.13 the black dotted curve indicates the theoretically achievable error rates with FEC and the green continuous line expresses the actual performance. It is evident that both of the curves match at higher SNR even though the simulated one start from a lower point. This phenomena may be labelled as the inherent error of rounding in each iteration which is done to speed up the simulation and save memory. In higher SNR and higher iterations the rounding becomes negligible hence the actual curve converges with

the theoretical one. In theorical curve there is no rounding so we get a smooth converging curve as expected.

Both small scale and large scale fading has effect on the algorithm which also affects both of the configurations. But this effect is not apparent from this graph. Nevertheless these fadings are always incorporated and has to be offset at the receiver.

A similar approach is taken while simulating the noncoherent or differential configuration. Unlike the coherent configuration in noncoherent the channel phase and other realization factors are neither known by the receiver and neither by the transmitter. So the receiver has to depend on the channel statistics to accurately recover the transmitted signal with minimal error. As mentioned elsewhere in this thesis, eventhough channel statistics is not needed for some estimators like the LS but it still can be incorporated into the algorithm however. And just so it will add some additional system overhead and some errors too in the overall statistics of utilizing this statistics of the coefficients effectively. The graph is shown below:

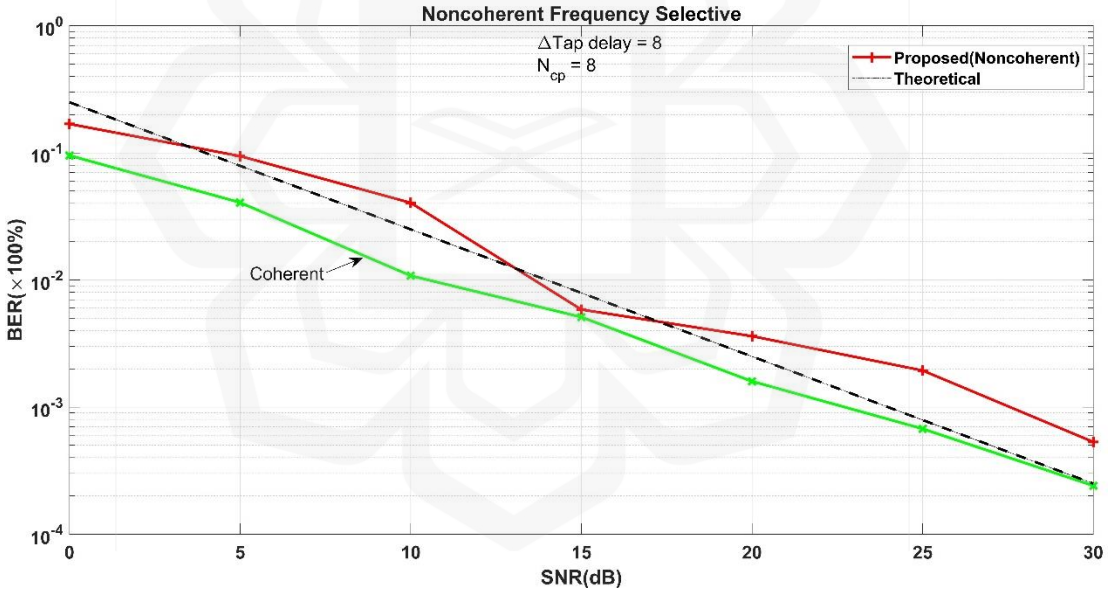

Figure 4.14 Simulation of the proposed algorithm in Noncoherent p2p configuration.

The coherent configuration curve was overlapped from the previous simulation for clarification purposes. From Figure 4.14 it can be seen that the noncoherent or differential configuration also has impressive performance and also begin to converge with the ideal theoretical curve in higher SNRs. The reason noncoherent curve has higher average error rate is caused by the additional error in the processing of the channel statistics. This additional error can still be further minimized with the help of other built-in Matlab functions. But usually the error caused by inefficient channel

statistics processing is unsubstantial compared to the overall error and this is overlooked usually.

It should be however mentioned that in more complex systems like the ones employing separate optimization algorithms this error can become substantial. In those cases however the statisticians already add some offsetting functions to keep the margin of error relatively small.

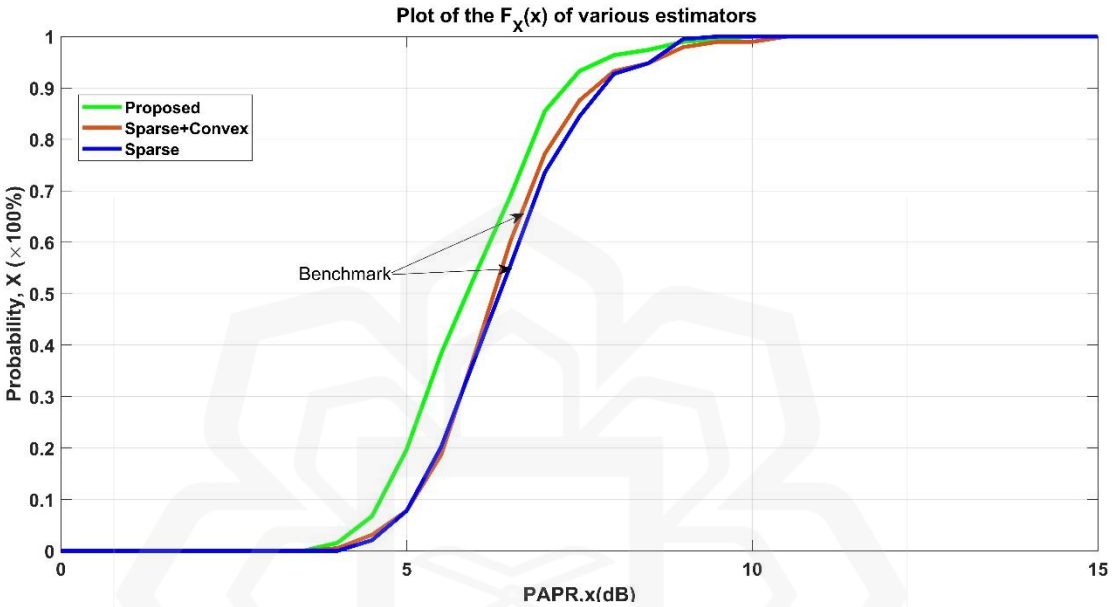

Figure 4.15 Plot of the CDF of different estimators against PAPR

The peak to average power ratio or PAPR is a very important metric to judge the efficiency of any wireless system. As we know a smaller value means that the amplifier in the transmitter can work more efficiently with a smaller overhead on the user interface. However it is interesting for another reason that is to see how the cumulative distribution function or CDF response in a given operating region under different estimators. In Figure 4.15 such a graph is shown.

It can be seen that the prosed model works just as fine and has an almost similar response to compressed sensing methods using sparse representation. In fact from Figure 4.15 it can also be interpreted that using a separate optimization algorithm such as the convex optimizer will still yield a similar performance as the proposed model. This further corroborates our objective 3 which was to analysis and compare our proposed model against CS based methods that may use optimization algorithms.

The CDF has a few derived functions which can also be plotted against the PAPR range. A few common functions from this category are the Folded CDF and the

Tail distribution CDF. It should be mentioned here that the CDF and it's derivatives can have a lot of cases where the variables are not identical i.g they're complex or dependant on other functions. For the Figure 4.15 only the general case was shown for the sake of simplicity.

In the next simulation the total no of bits were changed to see how overall the CDF changes as more bits are added to the transmitted signal. Theoretically when more bits are added the resulting curve should be flatter as the distribution should be more evenly distributed. The resulting graph is below:

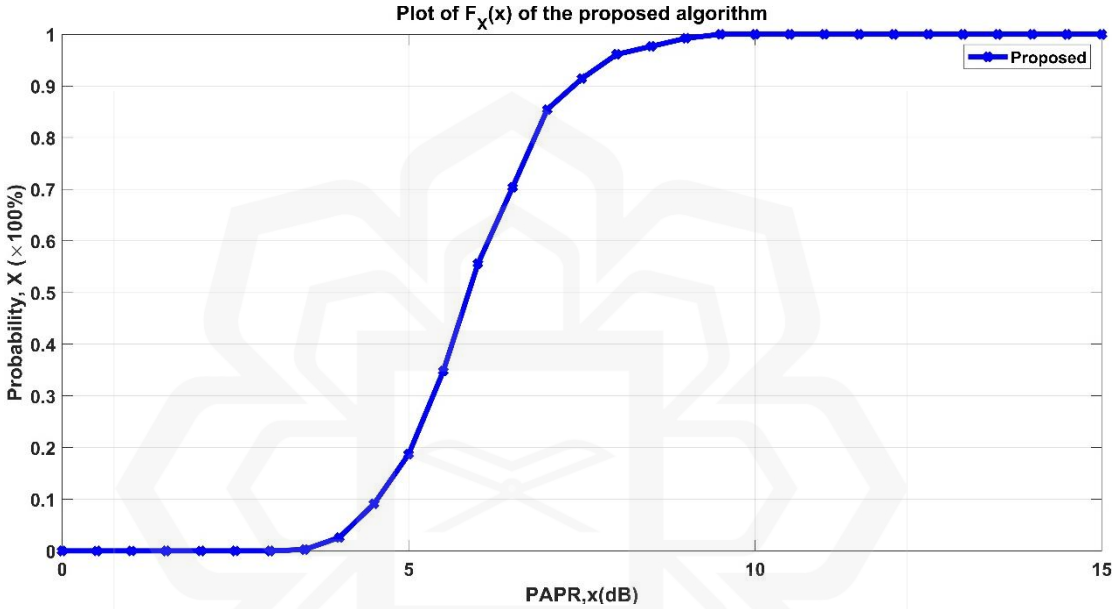

Figure 4.16 Plot of CDF of the proposed model.

It may not be so apparent from Figure 4.16 but if we compare point to point with previous Figure 4.17 we can see that in similar PAPR range the responses here are much more flatter spread. This is partly because the increased no of bits to be estimated using the algorithm increases the overall probability of an accurate estimation. And since the algorithm uses dual residue functions a two fold increase in the number of transmitted bits results in a proportional increase in estimation accuracy.

The plot also shows that the cumulative distribution function eventhough not heavily affected by changes in no of bits or bits/symbol, it does show a improved response which may well be in the benefit of large industrial transmitters. This is because unlike the experimental cases in industrial cellular networks the transmitters and receivers has to deal with huge chunks of sybols which adds up the error. Hence a

incremental CDF means that the estimation performance will not fall bellow the defined standard.

It can be concluded now from the previous 4 simulations that the proposed model doesn't require a separate optimization algorithm to generate similar results. These simulations were all done comparing with the benchmark algorithm that uses convex optimization which utilizes sparsity of the mmwave channel.

To summarize the previous 4 results, it can be said that even though optimization algorithms are beneficial if we intend to estimate sparse signals; it's not essential for the proposed model. It should be bear in mind that optimization algorithms like the convex one still can be used of course, but it may require further offsetting since these algorithms add some noise with their estimation process. To summarize the results, we can look at the table below:

Table 4-1 Comparison results between convex algorithm and the proposed model.

Parameter	**Action**	**Observation**
Subcarrier	Halved	The proposed model works better. The higher the SNR the more obvious the performance becomes
No of Taps	Doubled	Flattens both of the curves. The variance is reduced so is the response from the curvesm. The proposed model clearly shows much les BER.
Doppler Frequency	Increased 5 fold	No comparable difference. Has the similar kind of response while the subcarrier was halved.
Overall	-	Comparing 1 factor at a time, the proposed model outperforms the benchmark in all cases.

In the above simulations, only 1 factor was changed at a time because it's technically not possible to simulate multiple parameters using the abovementioned algorithms. A 3D plot may be derived but using the convex optimization model which has a separate algorithm for helpting function itself; it not possible using the user's operating system configuration.

All of the simulations above support the research objectives. The figures in the beginning show direct improvements of the proposed algorithm over benchmark and the latter ones are supporting graphs that corroborates the assumed outcomes. For a brief outlook, all the figures in this chapter and their corresponding objectives are mentioned here:

Table 4-2 Simulation results & their corresponding objectives.

Figure No.	Corresponding Objectives	Remarks
4.1	1,2	MSE improved
4.2	1,2	BER improved
4.3	1,2	PER improved
4.4	2,3	SER improved
4.5	3	Adaptibility increased
4.6	2,3	Comparison with CS method
4.7	2	Comparison in sub-standard scenarios
4.8	2,3	Double-Tap comparison
4.9	1,2,3	Frequency response
4.10	2,3	Rician profile analysis
4.11	2,3	Weibull profile analysis
4.12	2,3	Nakagami profile analysis
4.13	2,3	Coherent P2P analysis
4.14	2,3	Differential P2P analysis
4.15	1,2,3	CDF analysis
4.16	1,2	CDF analysis

It should be noted that the purpose of Table 4.2 is to demonstrate the relativity of the objectives and the simulations. The elaborated explanations were provided after the respective simulations.

Due to the resource constraints of the system and lab facilities; the no of graphs and simulations were kept as many as possible. Like abovementioned, the convex optimization algorithm uses several dedicaed calculating functions which require immense computing power that maybe only available in a working super computer. Nonetheless, the already provided simulations sufficiently proves the superiority of the proposed algorithm.

It should be noted that sudden rises and falls in the resulting carves can be regarded as outliers. Outliers are points in a graphs who are the most furthest from the fitting. Appropriate curve fitting may also be used to reduce these outliers. In any case, outliers never define the response of the curve but only the performance of the fitting. In the provided simulations no dedicated curve fitting algorithms were used for the sake fo simplicity and system resource.

For the similar reasons, the range of the SNRs are kept in the standard zone because any further range are not the subject of this discussion and also doesn't effect the analysis of the results. Also in majority of scholarly articles the simulations zone is usually kept from 10dB-30dB. For this reason it's easier to benchmark any analysis because they are all in the commercial operating range.

A few parameters weren't changed at all during any of the analysis. The configuration of the pilot matrix is one of them. Pilot symbols aren't changed when they transmitted with the data symbols during a symbol period and they're predefined in most cases. It is to facilitate their detection and uncoding at the receiver. Although adaptive pilots are possible. But it will require additional processing at the receiver to offset the phase shifts to properly differentiate the pilot from the data blocks. In the later 5G releases starting from 5G NR a new subcarrier structure was proposed. This structure involved further space for control channels and data channels which rendered the need of adaptive pilots surplus.

4.3 CHAPTER SUMMARY

In this chapter, several simulations were shown on the proposed scheme. The MSE comparison is used to judge the mean distance between the ideal and obtained curves in terms of square units. The BER is an overall indicator of estimator performance. Packet error rate comparison is useful when different estimators are compared in data blocks instead of units. It was also shown that the SER curve of different minimization techniques could vary depending on the method of channel state acquisition. To display the performance advantage of the proposed formula, we also showed an F-OFDM implementation which also showed a promising result. There are still some potential aspects though in this technique which is discussed in the following chapter

CHAPTER FIVE

CONCLUSION

5.1 INTRODUCTION

There are some limitations to the simulations used in this thesis work. For instance, technically, the no of iterations required to get the best result is infinite. But for obvious reasons, it isn't possible to get perfect results even if the algorithm is flawless. Not to mention, the speed of the simulation is also heavily dependent on the performing machine. For these common reasons, researchers usually take advantage of techniques like Monte Carlo simulations to get the probability distribution of the scheme's performance. Since channel estimation is heavily based on processing a large number of samples or bits in this case, when running these kinds of simulations, it is apparent to keep an eye on the process's time consumption of the process not only memory overhead.

5.2 RESULTS AND FUTURE WORKS

The objectives stated in Chapter 1 have been achieved in the sense that we assume one or few things for simplicity. And because of the lack of technology to test the proposed model, the thesis work will lack some of the practical aspects. Having said that, the author intends to bring the idea and importance of channel estimation in signal processing in light of the new features enabled by the fifth generation of cellular technology.

As for the first objective, which was to optimize the performance of the legacy pilot-based estimation techniques, it can be said, based on the results obtained, that the most common drawback of the legacy algorithm is the incorporation of random noise and the secondary channel statistics, namely the coefficient matrices. Both of these shortcomings have been addressed in the proposed algorithm as it employs intuitive, adaptive distance minimization and the adoption of weighted measurements. The results

in chapter five can also be apprehended that in the effective SNR range of cellular communication, the proposed algorithm performs fairly well compared with its legacy counterparts. Not to mention the effect Adaptively estimating the weight function can also speed up the cellular process, especially the connection setup and discharge. It should also be mentioned here that the purpose of the algorithm is to amend the existing limitations of these pilot-based algorithms, not to evolve them. As such, the proposed algorithm doesn't add any overhead but instead minimizes the overhead caused by adding redundancies in the algorithms.

The second objective was a comparative study against semi-blind or blind compressive sensing-based methods. From the simulation results, we can see in terms of performance (BER), the proposed method is close enough to be called an alternative to the complex CS-based methods. And, of course, in terms of simplicity and system overload, it is fundamental that since the proposed method doesn't use any separate optimization algorithm, it is fundamentally less resource-demanding. Of course, one can always pursue this as a potential aspect of further research with more parameters on focus.

The third objective was to estimate the RF channel adaptively instead of using fixed weights that are easier to calibrate but give poor results when there's an increasing number of subcarriers. As it was discussed in the previous chapter, adaptive weight was used to make the algorithm more fluid since it was shown that the likelihood of the packet and bit error rate is substantially reduced. And thus leading to a more robust and system friendly estimator.

5.3 CHAPTER SUMMARY

In this final chapter, the achievement and the future possibilities of this research work were discussed. It was also shown that a moderate complexity estimator with above-average performance is the best choice for the current 5G standards since it imparts much new functionality requiring more system resources. The adaptive algorithm boasts better performance than the legacy ones while keeping the complexity moderate. Although the performance aspect of the estimator was mainly focused on in this study,

a future study can be solely based on the statistical complexity reduction of this method which the author desired to leave for simplicity.

REFERENCES

Aboutorab, N., Hardjawana, W., & Vucetic, B. (2013). Application of compressive sensing to channel estimation of high mobility OFDM systems. IEEE International Conference on Communications, 4946–4950.

Ahmed, I., Khammari, H., Shahid, A., Musa, A., Kim, K. S., De Poorter, E., & Moerman, I. (2018). A survey on hybrid beamforming techniques in 5G: Architecture and system model perspectives. IEEE Communications Surveys and Tutorials, 20(4), 3060–3097.

Alkhateeb, A., El Ayach, O., Leus, G., & Heath, R. W. (2013, June 13). Hybrid precoding for millimeter wave cellular systems with partial channel knowledge. 1–5.

Alkhateeb, Ahmed, & Heath, R. W. (2016). Frequency Selective Hybrid Precoding for Limited Feedback Millimeter Wave Systems. IEEE Transactions on Communications, 64(5), 1801–1818.

Alkhateeb, Ahmed, Mo, J., González-Prelcic, N., & Heath, R. W. (2014). MIMO precoding and combining solutions for millimeter-wave systems. IEEE Communications Magazine, 52(12), 122–131.

Aminjavaheri, A., Farhang, A., RezazadehReyhani, A., & Farhang-Boroujeny, B. (2015). Impact of timing and frequency offsets on multicarrier waveform candidates for 5G. 2015 IEEE Signal Processing and Signal Processing Education Workshop, SP/SPE 2015, 178–183.

Basciftci, Y. O., Koksal, C. E., & Ashikhmin, A. (2018). Physical-Layer Security in TDD Massive MIMO. IEEE Transactions on Information Theory, 64(11), 7359–7380.

Beltran, F., Ray, S. K., & Gutiérrez, J. A. (2016). Understanding the Current Operation and Future Roles of Wireless Networks: Co-Existence, Competition and Co-Operation in the Unlicensed Spectrum Bands. IEEE Journal on Selected Areas in Communications, 34(11), 2829–2837.

Bjornson, E., De Carvalho, E., Sorensen, J. H., Larsson, E. G., & Popovski, P. (2017). A Random Access Protocol for Pilot Allocation in Crowded Massive MIMO Systems. IEEE Transactions on Wireless Communications, 16(4), 2220–2234.

Buzzi, S., Chih-Lin, I., Klein, T. E., Poor, H. V., Yang, C., & Zappone, A. (2016). A survey of energy-efficient techniques for 5G networks and challenges ahead. IEEE Journal on Selected Areas in Communications, 34(4), 697–709.

Dai, L., Wang, B., Peng, M., & Chen, S. (2019). Hybrid precoding-based millimetre-wave massive MIMO-NOMA with simultaneous wireless information and power transfer. IEEE Journal on Selected Areas in Communications, 37(1), 131–141.

Ding, T., Yuan, X., & Liew, S. C. (2019). Sparsity learning-based multiuser detection in grant-free massive-device multiple access. IEEE Transactions on Wireless Communications, 18(7), 3569–3582.

Feng, M., & Hong, J. (2020). An improved channel estimation algorithm based on DFT in the OFDM system. Proceedings - 2020 International Conference on Computer Information and Big Data Applications, CIBDA 2020, 321–325.

Ghosh, A., Maeder, A., Baker, M., & Chandramouli, D. (2019). 5G Evolution: A View on 5G Cellular Technology Beyond 3GPP Release 15. IEEE Access, 7, 127639–127651.

Hamamreh, J. M., Ankarali, Z. E., & Arslan, H. (2018). CP-Less OFDM with Alignment Signals for Enhancing Spectral Efficiency, Reducing Latency, and Improving PHY Security of 5G Services. IEEE Access, 6, 63649–63663.

Hardjawana, W., Li, R., Vucetic, B., Li, Y., & Yang, X. (2010). A new iterative channel estimation for high mobility MIMO-OFDM systems. IEEE Vehicular Technology Conference.

Hemadeh, I. A., Satyanarayana, K., El-Hajjar, M., & Hanzo, L. (2018). Millimeter-Wave Communications: Physical Channel Models, Design Considerations, Antenna Constructions, and Link-Budget. IEEE Communications Surveys and Tutorials, 20(2), 870–913.

Hong, W., Baek, K. H., & Ko, S. (2017). Millimeter-Wave 5G Antennas for Smartphones: Overview and Experimental Demonstration. IEEE Transactions on Antennas and Propagation, 65(12), 6250–6261.

Kamel, M., Hamouda, W., & Youssef, A. (2016). Ultra-Dense Networks: A Survey. IEEE Communications Surveys and Tutorials, 18(4), 2522–2545.

Ketonen, J., Juntti, M., Ylioinas, J., & Cavallaro, J. R. (2013). Decision-Directed Channel Estimation Implementation for Spectral Efficiency Improvement in Mobile MIMO-OFDM. Journal of Signal Processing Systems 2013 79:3, 79(3), 233–245.

Ketonen, J., Juntti, M., Ylioinas, J., & Cavallaro, J. R. (2015). Decision-Directed Channel Estimation Implementation for Spectral Efficiency Improvement in Mobile MIMO-OFDM. Journal of Signal Processing Systems, 79(3), 233–245.

Kuai, X., Yuan, X., Yan, W., Liu, H., & Zhang, Y. J. (2019). Double-sparsity learning-based channel-and-signal estimation in massive MIMO with generalized spatial modulation. ArXiv, 68(5), 2863–2877.

Liu, D., Wang, L., Chen, Y., Elkashlan, M., Wong, K. K., Schober, R., & Hanzo, L. (2016). User Association in 5G Networks: A Survey and an Outlook. IEEE Communications Surveys and Tutorials, 18(2), 1018–1044.

Liu, Y., & Sezginer, S. (2011). Simple iterative channel estimation in LTE systems. 2011 8th International Workshop on Multi-Carrier Systems and Solutions, MC-SS 2011, 1–5.

Liu, Y., & Sezginer, S. (2012). Iterative compensated MMSE channel estimation in LTE systems. IEEE International Conference on Communications, 4862–4866.

Masud, M., & Kamal, M. (2010). Adaptive Channel Estimation Techniques for MIMO OFDM Systems. International Journal of Advanced Computer Science and Applications, 1(6).

Mohammadreza Rouzegar, S., & Spagnolini, U. (2017). Channel estimation for diffusive mimo molecular communications. ArXiv, 67(7), 4872–4884.

Pan, P., Wang, H., Shen, L., & Lu, C. (2019). Equivalence of Joint ML-Decoding and Separate MMSE-ML Decoding for Training-Based MIMO Systems. IEEE Access, 7, 178862–178869.

Qin, Q., Gui, L., Cheng, P., & Gong, B. (2018). Time-varying channel estimation for millimeter wave multiuser MIMO systems. IEEE Transactions on Vehicular Technology, 67(10), 9435–9448.

Rappaport, T. S., Xing, Y., MacCartney, G. R., Molisch, A. F., Mellios, E., & Zhang, J. (2017). Overview of Millimeter Wave Communications for Fifth-Generation (5G) Wireless Networks-With a Focus on Propagation Models. IEEE Transactions on Antennas and Propagation, 65(12), 6213–6230.

Rouzegar, S. M., & Spagnolini, U. (2017). Channel estimation for diffusive MIMO molecular communications. EuCNC 2017 - European Conference on Networks and Communications.

Shafi, M., Molisch, A. F., Smith, P. J., Haustein, T., Zhu, P., De Silva, P., … Wunder, G. (2017). 5G: A tutorial overview of standards, trials, challenges, deployment, and practice. IEEE Journal on Selected Areas in Communications, 35(6), 1201–1221.

Singh, P., Mishra, H. B., Jagannatham, A. K., & Vasudevan, K. (2019a). Estimation Schemes for MIMO-FBMC-OQAM Systems. 67(18), 4668–4682.

Singh, P., Mishra, H. B., Jagannatham, A. K., & Vasudevan, K. (2019b). Semi-Blind, Training, and Data-Aided Channel Estimation Schemes for MIMO-FBMC-OQAM Systems. IEEE Transactions on Signal Processing, 67(18), 4668–4682.

Sohrabi, F., & Yu, W. (2017). Hybrid Analog and Digital Beamforming for mmWave OFDM Large-Scale Antenna Arrays. IEEE Journal on Selected Areas in Communications, 35(7), 1432–1443.

Sun, S., Rappaport, T. S., Thomas, T. A., Ghosh, A., Nguyen, H. C., Kovacs, I. Z., Partyka, A. (2016). Investigation of Prediction Accuracy, Sensitivity, and Parameter Stability of Large-Scale Propagation Path Loss Models for 5G Wireless Communications. IEEE Transactions on Vehicular Technology, 65(5), 2843–2860.

Uwaechia, A. N., Mahyuddin, N. M., Ain, M. F., Abdul Latiff, N. M., & Za'bah, N. F. (2019). On the Spectral-Efficiency of Low-Complexity and Resolution Hybrid Precoding and Combining Transceivers for mmWave MIMO Systems. IEEE Access, 7, 109259–109277.

van de Beek, J. J., Edfors, O., Sandell, M., Wilson, S. K., & Borjesson, P. O. (1995). On channel estimation in OFDM systems. IEEE Vehicular Technology Conference, 2(1), 815–819.

Venugopal, K., Alkhateeb, A., Gonzalez Prelcic, N., & Heath, R. W. (2017). Channel Estimation for Hybrid Architecture-Based Wideband Millimeter Wave Systems. IEEE Journal on Selected Areas in Communications, 35(9), 1996–2009.

Wang, B., Gao, F., Jin, S., Lin, H., & Li, G. Y. (2018). Spatial- and frequency-wideband effects in millimetre-wave massive MIMO systems. IEEE Transactions on Signal Processing, 66(13), 3393–3406.

Wang, W., Cheng, N., Teh, K. C., Lin, X., Zhuang, W., & Shen, X. (2019). On Countermeasures of Pilot Spoofing Attack in Massive MIMO Systems: A Double Channel Training Based Approach. IEEE Transactions on Vehicular Technology, 68(7), 6697–6708.

Xiao, M., Mumtaz, S., Huang, Y., Dai, L., Li, Y., Matthaiou, M., … Ghosh, A. (2017). Millimeter Wave Communications for Future Mobile Networks. IEEE Journal on Selected Areas in Communications, 35(9), 1909–1935.

Yilmaz, B. B., & Erdogan, A. T. (2019). Compressed training-based massive MIMO. IEEE Transactions on Signal Processing, 67(5), 1191–1206.

Zhang, J., Ge, X., Li, Q., Guizani, M., & Zhang, Y. (2017, October 2). 5G millimetre-wave antenna array: Design and challenges. IEEE Wireless Communications, 24(2), 106-112.

Zhang, J., Yuan, X., & Zhang, Y. J. A. (2018). Blind Signal Detection in Massive MIMO: Exploiting the Channel Sparsity. IEEE Transactions on Communications, 66(2), 700–712.

APPENDIX 1: MATLAB CODES

1. OFDM system BER

```
clc;
cd '(File directory)'
```

// Define parameters //

```
m=input() ;
N=input() ;
M=input() ;
pilotFrequency=input() ;
E=input();
Ncp=input() ;
L=input();
typ=input();
```

// Dataset generation //

```
D=randi ([0 M-1],m,N);
```

// Defining Tx,Rx //

```
switch typ
    case 1
        Tx=qammod(D,M);
        Rx=qamdemod(D,M);
    case 2
        Tx=pskmod(D,M);
        Rx=pskdemod(D,M);
    otherwise
        error('Error, Constellation not found!');
end
```

// Mapping //

```
D_Mod = Tx;
```

// Series to parallel conversion //

```
D_Mod_serial=D_Mod.';
```

// Defining pilot & data locations //

```
PLoc = 1:pilotFrequency:N;
DLoc = setxor(1:N,PLoc);
```

// Insert pilots //

```
D_Mod_serial(PLoc,:)=E*D_Mod_serial(PLoc,:);
```

```
figure;
imagesc(abs(D_Mod_serial ))
```

// IFFT //

```
d_ifft=ifft(D_Mod_serial);
```

// Parallel to series //

```
d_ifft_parallel=d_ifft.';
```

// CP addition //

```
CP_part=d_ifft_parallel(:,end-Ncp+1:end);
ofdm_cp=[CP_part d_ifft_parallel];
```

// Channel generation //

```
h= randn(1,L) + 1j * randn(1,L);
h = h./norm(h);
H = fft(h,N);
d_channelled = filter(h,1,ofdm_cp.').';
channel_length = length(h);
H1_power_dB = 10*log10(abs(H.*conj(H)));
```

// Add AWGN //

```
count=0;
snr_vector=0:4:40;
for snr=snr_vector
    SNR = snr + 10*log10(log2(M));
    count=count+1 ;
    disp(['step: ',num2str(count),' of: ',num2str(length(snr_vector))])
    ofdm_noisy_NoCH=awgn(ofdm_cp,SNR,'measured' ) ;
    ofdm_noisy_with_chann=awgn(d_channelled,SNR,'measured' ) ;
```

// Data reception //

```
cp_removed_NoCH=ofdm_noisy_NoCH(:,Ncp+1:N+Ncp);
cp_removed_with_chann=ofdm_noisy_with_chann(:,Ncp+1:N+Ncp);
parallel_NoCH=ofdm_cp_removed_NoCH.';
parallel_chann=ofdm_cp_removed_with_chann.';
```

// FFT //

```
parallel_fft_NoCH=fft(parallel_NoCH) ;
parallel_fft_channel=fft(parallel_chann) ;
```

// Channel estimation //

```
    TxP = D_Mod_serial(PLoc,:);
    RxP = parallel_fft_channel(PLoc,:);
    Hpilot_LS= RxP./TxP;
```

```
    for r=1:m
        H_MMSE(:,r) = MMSE(RxP(:,r),TxP(:,r),N,pilotFrequency,h,SNR);
    end
    for q=1:m
    HData_LS(:,q) = interpolate(Hpilot_LS(:,q).',PLoc,N,'spline');
    end
```

// Parallel to series //

```
LS_parallel1=HData_LS.';
MMSE_parallel1=H_MMSE.';
```

// De-map //

```
received_NoCH=demod(Rx,(parallel_fft_NoCH.'),1000) ;
received_chann_LS=demod(Rx,(parallel_fft_channel.')./HData_LS_parallel1)
;
received_chann_MMSE=demod(Rx,(parallel_fft_channel.')./(HData_MMSE_paral
lel1)) ;
```

// Removing data //

```
no_pilots=D(:,DLoc);
Rec_d_NoCH=received_NoCH(:,DLoc);
Rec_d_LS=received_chann_LS(:,DLoc);
Rec_d_MMSE=received_chann_MMSE(:,DLoc);
```

// BER calculation //

```
[~,r_NoCH(count)]=symerr(D_no_pilots,Rec_d_NoCH) ;
[~,r_LS(count)]=symerr(D_no_pilots,Rec_d_LS) ;
[~,r_MMSE(count)]=symerr(D_no_pilots,Rec_d_MMSE) ;
end
figure;
semilogy(snr_vector,r_NoCH,'-+');hold on
semilogy(snr_vector,r_LS,'-o');
semilogy(snr_vector,r_MMSE,'-s');
grid ;
hold off;
H_power_esti_dB_LS     =
10*log10(abs(HData_LS_parallel1.*conj(HData_LS_parallel1)));
H_power_esti_dB_MMSE     =
10*log10(abs(HData_MMSE_parallel1.*conj(HData_MMSE_parallel1)));
figure;hold on;
plot(H_power_dB(1:8:end),'+k','LineWidth',3);
plot(H_power_esti_dB_LS(1,(1:8:end)),'or','LineWidth',3);
plot(H_power_esti_dB_MMSE(1,(1:8:end)),'Sb','LineWidth',1);
 title('Real time and Estimated');
    xlabel('Time');
    ylabel('Magnitude');
```

2. MSE calculation for MMSE vs MSE perspective

// Define parameters and indices //

```
clc;

num_samples=500;
lamda = 1;

constrain = 'L2';
x=rand(1,num_samples);
m=5;
b=-2;

ya=m*x + b;
SNR=10;
y=awgn(ya,SNR);

epochs = 1000;
mm=randn();
bm=randn();
eta=2e-4;
ym=mm*x + bm;

e=y-ym;
E=mean(e.^2);
```

// Load Tx //

```
for i=1:epochs
    mm=mm + 2*eta*x*e';
    if(strcmp(constrain,'L1'))
        mm = mm - 2*eta*lamda*mm./abs(mm);
        if(lamda>0)
            lamda = lamda - eta*abs(mm);
        end
    elseif(strcmp(constrain,'L2'))
        mm = mm - 2*eta*lamda*mm;
        if(lamda>0)
            lamda = lamda - eta*mm.^2;
        end
    end
    bm=bm + 2*eta*sum(e);
    ym=mm*x + bm;
    e=y-ym;
    E=[E mean(e.^2)];
    E2=[E mean(e.^2.1)];
end
```

// Plot dataset //

```
hold on;

plot(10*log10(E))
plot(14*log10(E))


grid minor
hold off;
```

```
[m b 0;mm bm lamda]
```

3. Rician flat channel interpretation

// Defining matrices //

```
EbNo = 0:60;
K = [4.0; 0.6];
M = [4; 8; 16; 64; 256];
```

// Interpolation and modulation //

```
for k = 1:length(K)
    for m = 1:length(M)
        mess = randi([0, M(m)-1], 100000, 1);
        if M(m) >= 16
            mod_mess = qammod(mess, M(m), pi/4, 'gray');
            ric_bit(:, m, k) = berfading(EbNo,'qam',M(m),1,K(k));
        else
            mod_mess = pskmod(message, M(m), pi/4, 'gray');
            ric_bit(:, m, k) = berfading(EbNo, 'psk', M(m), 1, K(k));
        end
        Es = mean(abs(mod_msg).^2);
        No = Es./((10.^(EbNo./10))*log2(M(m)));

        h = sqrt( K(k)/(K(k)+1)) +...
        sqrt( 1/(K(k)+1))*(1/sqrt(2))*(randn(size(mod_msg))...
         + 1j*randn(size(mod_msg)));
        ric_msg = mod_msg.*h;

        for c = 1:100
             for jj = 1:length(EbNo)
                nois_mod = ric_mess +...
                sqrt(No(jj)/2)*(randn(size(mod_mess))+...
                1j*randn(size(mod_mess))); %AWGN
                nois_mod = nois_mod ./ h;
                if M(m) >= 16
                    demod_mess = qamdemod(nois_mod, M(m), pi/4, 'gray');
                else
                    demod_mess = pskdemod(nois_mod, M(m), pi/4, 'gray');
                end
                [number,BER(c,jj)] = bit_e(mess,demod_mess);
            end
        end
        sum_bit(:,m, k) = sum(BER)./c;
    end
end
```

// Data plotting //

```
figure(1)

semilogy(EbNo, sum_bit(:,1,1), 'b-o', EbNo, sum_bit(:,2,1), 'r-o',...
EbNo, sum_bit(:,3,1), 'g-o', EbNo, sum_bit(:,4,1), 'c-o',...
EbNo, sum_bit(:,5,1), 'k-o',...
```

```
EbNo, ric_bit(:,1,1), 'b-', EbNo, ric_bit(:,2,1), 'r-',...
EbNo, ric_bit(:,3,1), 'g-', EbNo, ric_bit(:,4,1), 'c-',...
EbNo, ric_bit(:,5,1), 'k-', 'LineWidth', 1.5)
grid on

figure(2)

semilogy(EbNo, sum_bit(:,1,2), 'b-o', EbNo, sum_bit(:,2,2), 'r-o',...
EbNo, sum_bit(:,3,2), 'g-o', EbNo, sum_bit(:,4,2), 'c-o',...
EbNo, sum_bit(:,5,2), 'k-o',...
EbNo, ric_bit(:,1,2), 'b-', EbNo, ric_bit(:,2,2), 'r-',...
EbNo, ric_bit(:,3,2), 'g-', EbNo,ric_bit(:,4,2), 'c-',...
EbNo, ric_bit(:,5,2), 'k-','LineWidth', 1.5)
grid on
```

4. OFDM system initialization

// Defining funcions //

```
OFDM.N=input();
OFDM.m=input();
OFDM.M=input();
OFDM.L=input();
OFDM.PoQ=input();
OFDM.Phase_Off=input();
OFDM.Symbol=input();
OFDM.Ncp=input();
```

// Initializing baseband Tx,Rx //

```
if OFDM.Symbol == 1
    OFDM.Symbol = 'binary';
else
    OFDM.Symbol = 'gray';
end
if OFDM.PoQ == 1
    hTx =
comm.PSKModulator('M',OFDM.M,'PhaseOffset',OFDM.Phase_Off,'SymbolOrder',
OFDM.Symbol);
    hRx =
comm.PSKModulator('M',OFDM.M,'PhaseOffset',OFDM.Phase_Off,'SymbolOrder',
OFDM.Symbol);
else
    hTx =
modem.qammod('M',OFDM.M,'PhaseOffset',OFDM.Phase_Off,'SymbolOrder',OFDM.
Symbol);
    hRx =
modem.qamdemod('M',OFDM.M,'PhaseOffset',OFDM.Phase,'SymbolOrder',OFDM.Sy
mbol);
end
```

// Data generation, mapping & sampling //

```
OFDM.dat=randi([0 OFDM.M-1],OFDM.m,OFDM.N/OFDM.L);
OFDM.map=modulate(hTx,OFDM.DATA);
```

```
OFDM.parallel=OFDM.map.';
OFDM.upsampled=upsample(OFDM.parallel,OFDM.L);
ofdm.am=ifft(OFDM.upsampled,OFDM.N);
ofdm.serial=ofdm.am.';
ofdm.CP_part=ofdm.serial(:,end-OFDM.Ncp+1:end);
ofdm.cp=[ofdm.CP_part ofdm.serial];
```

// Rx initializing //

```
SNRstart=0;
SNRincrement=4;
SNRend=30;
c=0;
r=zeros(size(SNRstart:SNRincrement:SNRend));
for snr=SNRstart:SNRincrement:SNRend
    c=c+1;
    ofdm.noisy=awgn(ofdm.cp,snr,'measured');
    ofdm.cpr=ofdm.noisy(:,OFDM.Ncp+1:OFDM.N+OFDM.Ncp); %remove the
Cyclic prefix
    ofdm.parallel=ofdm.cpr.';
    OFDM.ademod=fft(ofdm.parallel,OFDM.N);
OFDM.downsampled=downsample(OFDM.amdemod,OFDM.L);
    OFDM.rserial=OFDM.downsampled.';
    OFDM.Umap=demodulate(hRx,OFDM.rserial);
    [n, r(c)]=symerr(OFDM.DATA,OFDM.Umap);
    disp(['SNR = ',num2str(snr),' step: ',num2str(c),' of
',num2str(length(r))]);
end
```

// Plotting //

```
snr=SNRstart:SNRincrement:SNRend;
semilogy(snr,r,'-
ok','linewidth',2,'markerfacecolor','r','markersize',8,'markeredgecolor'
,'b');grid;
title('Error Rate vs SNR');
ylabel('SER');
xlabel('SNR [dB]');
legend(['SER N = ', num2str(OFDM.N),' ',num2str(hTx.M),'-',hTx.type]);
```

5. Visualizing spectrum

```
fprintf();

fileName = matfilename();
filePath = matfilename();
filePath = filePath(1:end-size(fileName, 2));

path(genpath([filePath 'files']), path);

fprintf();

guiMain;

fprintf();
```

```
clearvars fileName filePath
```

LIST OF PUBLICATIONS

Journal Papers:

Hasan, A., Motakabber, S. M. A., Anwar, F., Habaebi, M. H., & Ibrahimy, M. I. (2022). An adaptive channel estimation scheme based on redundancy minimization for filtered OFDM networks. *TELKOMNIKA (Telecommunication Computing Electronics and Control)* (Published) https://doi.org/10.12928/TELKOMNIKA.v21i1.24258

Hasan, A., Motakabber, S. M. A., Anwar, F., Habaebi, M. H., & Ibrahimy, M. I. (2021). Dual – Adaptive Redundancy Minimization Based Channel Estimation Method for MIMO OFDM Systems. *ASIAN JOURNAL OF ELECTRICAL AND ELECTRONIC ENGINEERING* (Published, Vol3 No.1, 2023) https://journals.alambiblio.com/ojs/index.php/ajoeee/article/view/42

Conference Proceedings:

Hasan, A., Motakabber, S. M. A., Anwar, F., Habaebi, M. H., & Ibrahimy, M. I. (2021). A Computationally Efficient Least Squares Channel Estimation Method for MIMO-OFDM Systems. *Proceedings of the 8th International Conference on Computer and Communication Engineering, ICCCE 2021*, 331–334. (Published) https://doi.org/10.1109/ICCCE50029.2021.9467142

Participations:

- 3 Minute Thesis (3MT) 2022 Winner
- 8th International Conference on Computer and Communication Engineering (ICCCE 2021)
- KERICE 2021

Supervisor